

**GENERALIZED GAS TURBINE ENGINE PERFORMANCE**

**BY**

**WILLIAM FRANCIS SCHMIDT**

GENERALIZED GAS TURBINE ENGINE PERFORMANCE

BY

WILLIAM FRANCIS SCHMIDT

A THESIS

SUBMITTED TO THE GRADUATE SCHOOL  
IN PARTIAL FULFILLMENT OF THE REQUIREMENTS  
FOR THE DEGREE OF MASTER OF SCIENCE

MECHANICAL ENGINEERING DEPARTMENT

WICHITA STATE UNIVERSITY

WICHITA, KANSAS

MAY, 1969

521021

## ACKNOWLEDGMENT

The author appreciates the counsel of his advisor, John B. Severt, and the encouragement and assistance provided by The Boeing Company through its Graduate Student Program.

TABLE OF CONTENTS

	PAGE
LIST OF TABLES . . . . .	iii
LIST OF FIGURES . . . . .	iv
NOMENCLATURE . . . . .	vi
INTRODUCTION . . . . .	ix
I. AIRPLANE MISSION ANALYSIS . . . . .	1
II. ENGINE CYCLE ANALYSIS . . . . .	6
III. ENGINE COMPONENT CHARACTERISTICS . . . . .	23
IV. GENERALIZED COMPUTER PROGRAM . . . . .	36
V. CONCLUSIONS AND RECOMMENDATIONS . . . . .	45
BIBLIOGRAPHY . . . . .	47

LIST OF TABLES

TABLE	PAGE
I. Engine Airflow Requirements . . . . .	5
II. Flow Continuity Matches for Front Fan Turbofan Engines . . .	14
III. Hardware Turbofan Engine Design Point Data	
Sea Level, Static, Standard Day . . . . .	40
IV. Design Point Data of Study Engines at	
Sea Level, Static, Standard Day . . . . .	43
V. Individual Design Point Data and Sizing Constants of	
Study Engines at Sea Level, Static, Standard Day . . . . .	44

## LIST OF FIGURES

FIGURE	PAGE
1. Turbine Engine Maximum Net Thrust . . . . .	2
2. Turbine Engine Cruise Performance . . . . .	3
3. Schematic Diagram of Front Fan Turbofan Engine . . . . .	7
4. Front Fan, Separate Exhaust, Turbofan Section Identification . . . . .	7
5. Schematic Diagram of Front Fan Turbofan Engine with Off-Design Iteration Loops . . . . .	13
6. Typical Fan Performance Map . . . . .	16
7. 10-Stage Axial-Flow Compressor Performance . . . . .	18
8. Turbine Performance Map . . . . .	20
9. Front Fan Turbofan Cycle Presented on Enthalpy- Entropy Diagram . . . . .	22
10. Eight-Stage Axial-Flow Compressor Map . . . . .	25
11. Modified (Two Transonic Stages) Eight-Stage Axial- Flow Compressor Performance . . . . .	26
12. Compressor Performance Comparison . . . . .	27
13. Experimental Combustor Data for Gasoline Burned in Air with Various Fuel-Air Ratios . . . . .	29
14. Turbine Performance Map . . . . .	32
15. Turbine Flow Characteristic . . . . .	33
16. Turbine Work Limit . . . . .	34
17. Turbine Efficiency . . . . .	35

FIGURE	PAGE
18. Typical Fan Performance Map Presented with Pressure Ratio Parameter . . . . .	37
19. Engine "A" (Front Fan) Sea Level Performance . . . . .	41
20. Engine "B" (Aft Fan) Sea Level Performance . . . . .	42

## NOMENCLATURE

<u>Symbol</u>	<u>Description</u>
BPR	Bypass ratio, fan duct airflow divided by primary airflow
c	Specific heat, Btu/lbm <sup>o</sup> R
C	Coefficient, e.g., velocity coefficient, etc.
CPR	Compressor pressure ratio, compressor outlet total pressure divided by compressor inlet total pressure
F	Thrust, propulsive force, lbf
FPR	Fan pressure ratio, fan outlet total pressure divided by fan inlet total pressure
g	Conversion factor, 32.174 lbm-ft/lbf-sec <sup>2</sup>
h	Specific enthalpy, Btu/lbm
K	Design constant
LHV	Fuel lower heating value, Btu/lbm
N	Rotor speed, rpm
P	Pressure, psia
Q	Pressure ratio parameter, $(CPR-1)/CPR_{stall}^{-1}$
R	Gas constant, 53.342 ft-lbf/lbm <sup>o</sup> R
s	Specific entropy, Btu/lbm- <sup>o</sup> R
SFC	Specific fuel consumption, $lbm_{fuel}/hr-lbf_{thrust}$
T	Temperature, <sup>o</sup> R
U	Rotor tip speed, ft/sec
V	Velocity, ft/sec
W	Weight flow rate, lbm/sec
γ	Specific heat ratio, $c_p/c_v$

<u>Symbol</u>	<u>Description</u>
---------------	--------------------

$\Gamma$	Referred flow, $W \sqrt{\theta/\delta}$ , lbm/sec
----------	---

$\delta$	Dimensionless pressure, $P/P_0$
----------	---------------------------------

$\Delta$	Increment or difference
----------	-------------------------

$\epsilon$	Function of $\gamma$ , $\frac{\gamma_0}{\gamma}$ X	$\left[ \frac{\left(\frac{\gamma+1}{2}\right)^{\frac{\gamma}{\gamma-1}}}{\left(\frac{\gamma_0+1}{2}\right)^{\frac{\gamma_0}{\gamma_0-1}}} \right]$
------------	--	--

$\eta$	Efficiency
--------	------------

$\theta$	Dimensionless temperature, $T/T_0$
----------	------------------------------------

Subscripts

a	Air
---	-----

am	Ambient
----	---------

B	Burner
---	--------

c	Compressor
---	------------

cr	Critical (at sonic conditions)
----	--------------------------------

f	Fan, fuel
---	-----------

FD	Fan duct
----	----------

g	Gas, gross
---	------------

j	Jet
---	-----

n	Net
---	-----

N	Number
---	--------

<u>Subscripts</u>	<u>Description</u>
p	Primary, pressure constant
r	Ram
t	Turbine
T	Total, stagnation condition
v	Velocity, volume constant
0	Airplane, free stream, NACA standard conditions
1	Inlet station, first rotor
2	Compressor or fan inlet station, second rotor
2.5	Compressor inlet station (front fan)
3	Compressor outlet station
3f	Fan duct inlet station
4	Turbine inlet station
4f	Fan duct outlet station, fan nozzle inlet station
5	Fan turbine inlet station
6	Fan turbine outlet station

### Superscripts

' Ideal, isentropic

### Dimensionless Quantities

$M_N$  Mach number, ratio of velocity to the acoustic velocity

## INTRODUCTION

Turbine aircraft engine performance can be accurately calculated using specific component performance maps for components that are compatibly sized. These data are limited to a particular engine and hence engine cycle. Generation of sufficient engine performance data for a parametric engine-aircraft study from individually matched components is therefore prohibitively costly in terms of both time and money.

This thesis develops methods of generalizing the performance of specific engine components for use in a generalized gas turbine engine performance computer program. This method produces inexpensive engine performance data for parametric studies.

Specific items treated in this thesis are:

1. The importance of considering engine cycle variations in airplane mission studies.
2. Engine cycle analysis techniques for off-design as well as design points. (Off-design iterations are not usually described in the literature and are extremely laborious without the assistance of a large digital computer.)
3. Accepted component performance presentations and methods of generalization.
4. The description, verification, and results of a generalized turbine engine performance computer program.

Previous investigators have generated "parametric" engine performance by using one or more of the following approximations:

1. Extrapolation of current hardware engine performance data.
2. Fixed operating line(s) on compressor and/or fan performance map(s).
3. Turbine nozzle(s) with choked (sonic) flow.
4. Constant component efficiencies.

None of these assumptions are valid over a very wide range of engine cycles or operating conditions.

The material for this thesis has been gleaned from unclassified U.S. Government, National Advisory Committee for Aeronautics (NACA/NASA) reports, technical society journals, and standard text books. Hardware engine performance was taken from the manufacturers' Model Specifications.

## CHAPTER I

### AIRPLANE MISSION ANALYSIS

The selection of an engine for an airplane depends on the aircraft's mission. However, the primary consideration is usually a minimization of installed engine plus fuel weight required for the desired aircraft flight. Breguet developed classical range and endurance equations that are functions of the airplane lift-drag polar, gross and final airplane weight, propulsive efficiency, and specific fuel consumption.<sup>1</sup> This calculation is easily adapted and optimized for airplanes with a single design point. However, most aircraft are multi-purpose and require a more detailed analysis that is especially suited to digital computers. This analysis usually consists of investigating individual engine cycles by:

1. Sizing the power plant to meet the airplane takeoff distance.
2. Calculating takeoff and climb-out fuel.
3. Determining aircraft range, endurance time or load carried over a given distance for a fixed gross weight.
4. Determining descent, hold, reserve, and landing fuel requirements.

The digital computer programs provide for multiple cruise or holding design points.

---

<sup>1</sup>Courtland D. Perkins and Robert E. Hage, Airplane Performance Stability and Control, pp. 183-194.

The main requirement for optimizing the engine cycle for a particular airplane is adequate engine performance data. An example of the effect of the engine cycle on airplane takeoff and cruise performance is illustrated by the following figures. These charts illustrate typical turbojet and turbofan engine performance at sea level takeoff and cruise flight conditions. Figure 1 illustrates the higher takeoff thrust lapse rate of turbofan engines compared to turbojets. This figure indicates that the installed static thrust of a turbofan engine in a given airplane would be greater than that of a turbojet for the same takeoff performance. For this simplified analysis, the engine is sized for constant thrust at the lift-off speed ( $0.2 M_N$  assumed).

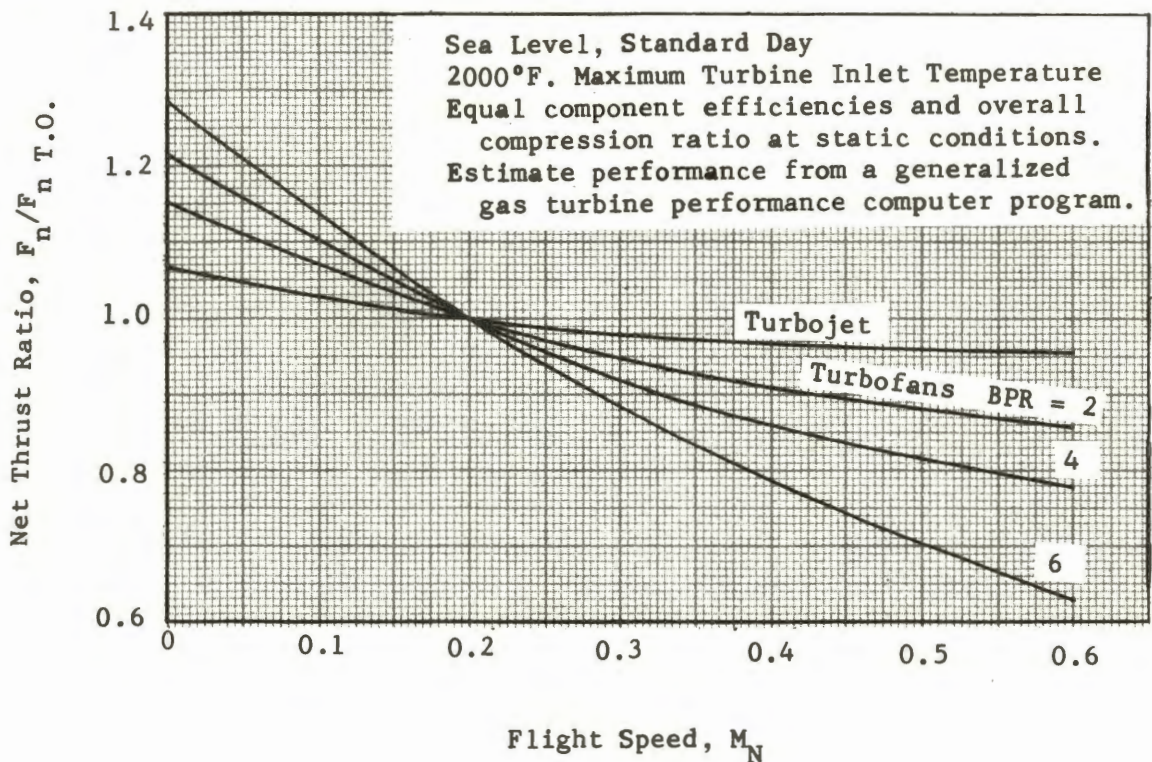


Figure 1. Turbine engine maximum net thrust

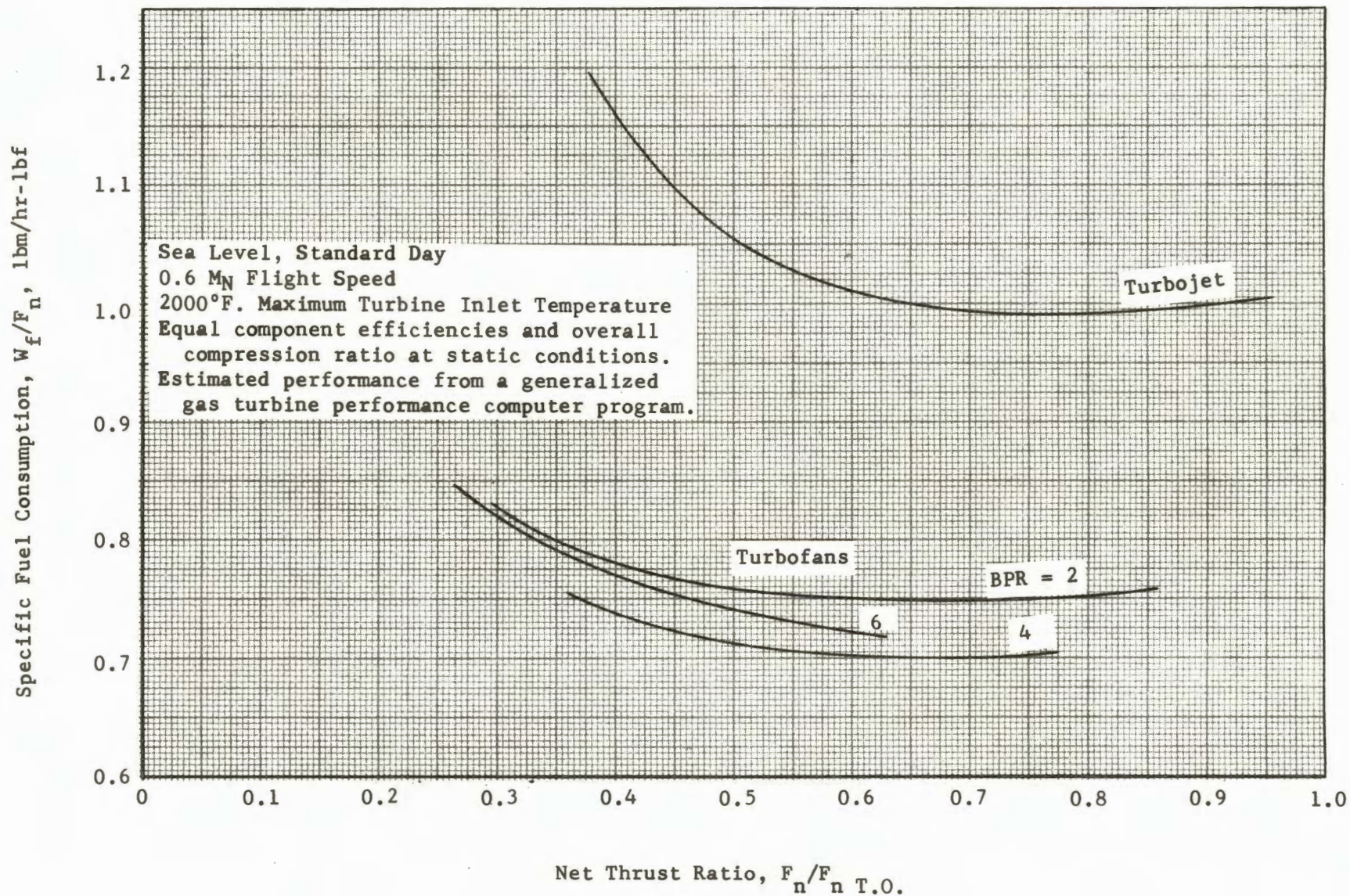


Figure 2. Turbine engine cruise performance

Figure 2 illustrates the wide variation in specific fuel consumption for airplane cruise at this flight condition ( $0.6 M_N$  at sea level). For example, an airplane that requires 40 percent take-off thrust for this flight condition would have a specific fuel consumption of 1.158 lb/hr-lb if a turbojet were used and 0.738 lb/hr-lb for a 4.0 bypass ratio turbofan. This 36 percent saving in fuel usage rate can be converted to additional endurance, range, or payload.

This abbreviated study indicates the advantages possible with a major engine cycle variation. More subtle advantages can be achieved by investigating other cycle variables at state-of-the-art component efficiencies and metallurgical temperature limits. Additional airplane design points could easily be investigated if engine performance data were available.

Secondary effects of engine weight and nacelle size can also be included in a more detailed study. Nacelle size can be approximated from airflow requirements. The relative sea level, static, standard day airflows required by the above engines for constant thrust at the takeoff condition are shown in Table I. Since the design point inlet diffuser Mach number is selected at a constant value, these flow ratios are actually area ratios. Engine diameters can be calculated from these area figures and weight and drag calculations can be completed.

TABLE I

## ENGINE AIRFLOW REQUIREMENTS

Bypass Ratio	Design Point Airflow Ratio
0	1.0
2	2.07
4	2.905
6	3.735

## CHAPTER II

### ENGINE CYCLE ANALYSIS

Gas turbine aircraft engines range from the relatively simple single rotor turbojet to the multiple rotor turboprop. Included in this array are various turbofan engine designs such as:

1. The conventional front fan that supercharges the primary compressor.
2. The aft fan formed as an extension of the fan turbine rotor.

The front fan turbofan cycle contains most of the elements of gas turbine engines so it will be used herein to describe the engine processes.

The general design point separate exhaust front fan turbofan engine cycle is illustrated schematically in Figure 3. Engine station numbers are depicted on the engine cross section of Figure 4. In this cycle, air is induced into the fan and compressed moderately. The air flow divides behind the fan into the bypass and primary flows. The bypass airflow passes around the main engine and is expanded through its nozzle to produce thrust. The primary flow is compressed further in the compressor, mixed with fuel and burned in the combustor, and expanded in the turbines and the primary exhaust nozzle. Work extracted by the turbines is used to drive the fan and compressor and the increased gas velocity in the nozzle provides additional thrust.

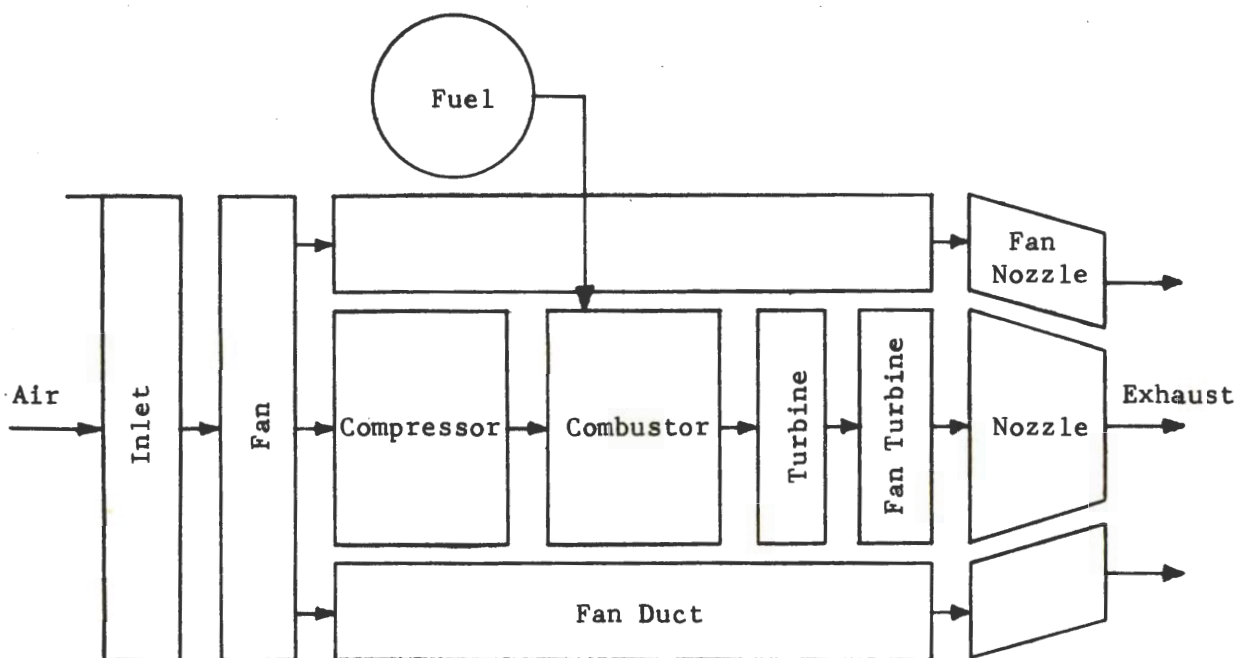


Figure 3. Schematic diagram of front fan turbofan engine

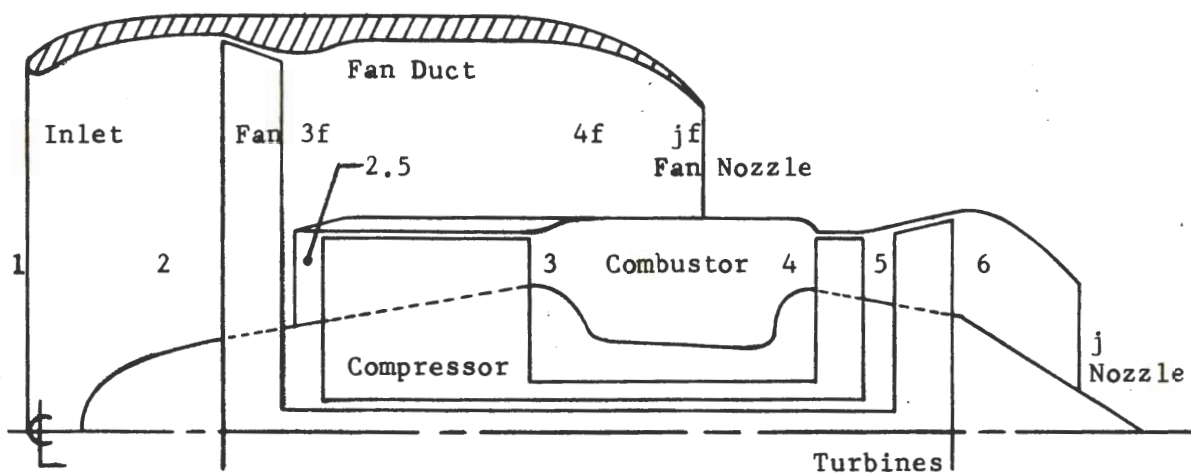


Figure 4. Front fan, separate exhaust, turbofan section identification

### Design Point Calculations

Design point cycle calculations are direct because the individual components' performance is specified. Control variables are calculated (sized) at the design point and used for off-design calculations.

Typical front fan turbofan engine design point calculations would be completed in the following manner.<sup>1</sup> Specific calculation details, available in the cited references, have been omitted for clarity.

Atmospheric conditions.  $P_{am}$  and  $T_{am}$  are selected or are a function of the selected flight altitude and a standard altitude table.

Inlet. The flight Mach number,  $M_o$ , and inlet diffuser efficiency,  $\eta_r$ , are specified.

$$T_{T2}/T_{am} = 1 + \frac{\gamma - 1}{2} M_o^2$$

$$P'_{T2}/P_{am} = (T_{T2}/T_{am})^{\gamma/(\gamma - 1)}$$

$$P_{T2}/P_{am} = \eta_r (P'_{T2}/P_{am})$$

$$F_r = W_{a2} V_o/g$$

---

<sup>1</sup>Franklin P. Durham, Aircraft Jet Powerplants, pp. 47-74.

Fan. Fan efficiency,  $\eta_f$ , pressure ratio, FPR, and flow,  $W_{a2}$ , are known.

Fan ideal work is calculated from the inlet conditions and the fan pressure ratio using isentropic relationships.

$$\Delta h'_f = f(\text{FPR}, T_{T2}) \quad (\text{isentropic relationship})$$

$$\Delta h_f = \Delta h'_f / \eta_f$$

$$h_{T2.5} = h_{T2} + \Delta h_f$$

$$T_{T2.5} = f(h_{T2.5}) \quad (\text{gas tables})^2$$

$$P_{T2.5} = P_{T2} (\text{FPR})$$

Fan duct.

$$T_{T3f} = T_{T2.5}$$

$$P_{T3f} = P_{T2.5}$$

Bypass ratio, BPR, and duct pressure drop,  $\Delta P_{FD}/P_{T3f}$ , are known.

$$W_{a3f} = (W_{a2}/(1 + \text{BPR})) \text{BPR}$$

$$P_{T4f} = P_{T3f} (1 - \Delta P_{FD}/P_{T3f})$$

$$T_{T4f} = T_{T3f}$$

---

<sup>2</sup> Joseph H. Keenan and Joseph Kaye, Gas Tables, pp. 1-33.

Fan nozzle. The fan nozzle efficiency,  $\eta_{fn}$ , or velocity coefficient,  $C_{vf}$ , is specified.

$$V'_{jf} = f (P_{T4f}/P_{jf}, T_{T4f}) \quad (\text{isentropic relationship})$$

$$V_{jf} = C_{vf} V'_{jf}$$

$$F_{gf} = W_{a3f} V_{jf}/g + A_{jf} (p_{jf} - P_{am})$$

Where  $A_{jf}$  is sized for  $W_{a3f}$  and  $p_{jf}$  is determined by nozzle calculations.

Compressor. Compressor efficiency,  $\eta_c$  and pressure ratio, CPR, are known.

$$\Delta h'_c = f (\text{CPR}, T_{T2.5}) \quad (\text{isentropic relationship})$$

$$\Delta h_c = \Delta h'_c / \eta_c$$

$$h_{T3} = h_{T2.5} + \Delta h_c$$

$$T_{T3} = f (h_{T3})$$

$$P_{T3} = P_{T2.5} (\text{CPR})$$

Combustor. Combustion efficiency,  $\eta_B$ , pressure drop,  $\Delta P_B/P_{T3}$ , fuel lower heating value, LHV, and turbine inlet temperature,  $T_{T4}$ , are known.

The fuel flow,  $W_f$ , or fuel air ratio,  $W_f/W_{a3}$ , is calculated from an energy balance.

$$\frac{W_f}{W_a} = \frac{h_{T4} - h_{T3}}{\eta_B (\text{LHV}) - h_{T4}} \quad (\text{neglecting enthalpy of incoming fuel and turbine cooling airflow})$$

$$W_{g4} = 1 + (W_f/W_a) W_{a3}$$

$$P_{T4} = P_{T3} (1 - \Delta P_B/P_{T3})$$

Turbine. The turbine efficiency,  $\eta_t$ , is known. It is also specified that the turbine must drive the compressor.

$$\Delta h_t = \Delta h_c (W_{a2.5}/W_{g4})$$

$$\Delta h'_t = \Delta h_t / \eta_t$$

$$P_{T4}/P_{T5} = f(\Delta h'_t, T_{T4}) \quad (\text{isentropic relationship})$$

$$P_{T5} = P_{T4} / (P_{T4}/P_{T5})$$

$$h_{T5} = h_{T4} - \Delta h_t$$

$$T_{T5} = f(h_{T5})$$

$$W_{g5} = W_{g4}$$

Fan Turbine. The fan turbine efficiency,  $\eta_{ft}$ , is known and this turbine drives the fan.

$$\Delta h_{ft} = \Delta h_f (W_{a2}/W_{g5})$$

$$\Delta h'_{ft} = \Delta h_{ft} / \eta_{ft}$$

$$P_{T5}/P_{T6} = f(\Delta h'_{ft}, T_{T5}) \quad (\text{isentropic relationship})$$

$$P_{T6} = P_{T5}/(P_{T5}/P_{T6})$$

$$h_{T6} = h_{T5} - \Delta h_{ft}$$

$$T_{T6} = f(h_{T6}) \quad (\text{gas tables})$$

$$W_{g6} = W_{g5}$$

Primary exhaust nozzle. The nozzle efficiency,  $\eta_j$ , or velocity coefficient,  $C_v$ , is specified:

$$V'_j = f(P_{T6}/P_j, T_{T6}) \quad (\text{isentropic relationship})$$

$$V_j = C_v V'_j$$

$$F_{gp} = \frac{W_{g6}}{g} V_j + A_j (P_j - P_{am})$$

where  $A_j$  is sized for  $W_{g6}$  and  $P_j$  is determined by nozzle calculations.<sup>3</sup>

External performance. Total gross thrust,  $F_g$ , net thrust,  $F_n$ , fuel flow,  $W_f$ , and specific fuel consumption, SFC, are calculated as:

$$F_g = F_{gf} + F_{gp}$$

$$F_n = F_g - F_r$$

$$W_f = (W_f/W_{a3}) W_{a3}$$

$$\text{SFC} = W_f / F_n$$

---

<sup>3</sup>Durham, op. cit., pp. 201-212.

### Off-design Calculations

Off-design engine performance calculations are iterative. The individual component hardware is specified for the design point and must be matched for flow continuity and work at off-design conditions. The iteration loops for the front fan turbofan engine are shown on the block diagram of Figure 5. The engine parameters indicated on Figure 5 are used to match flow requirements between the components. Specific matches and controlling parameters are indicated in Table II.

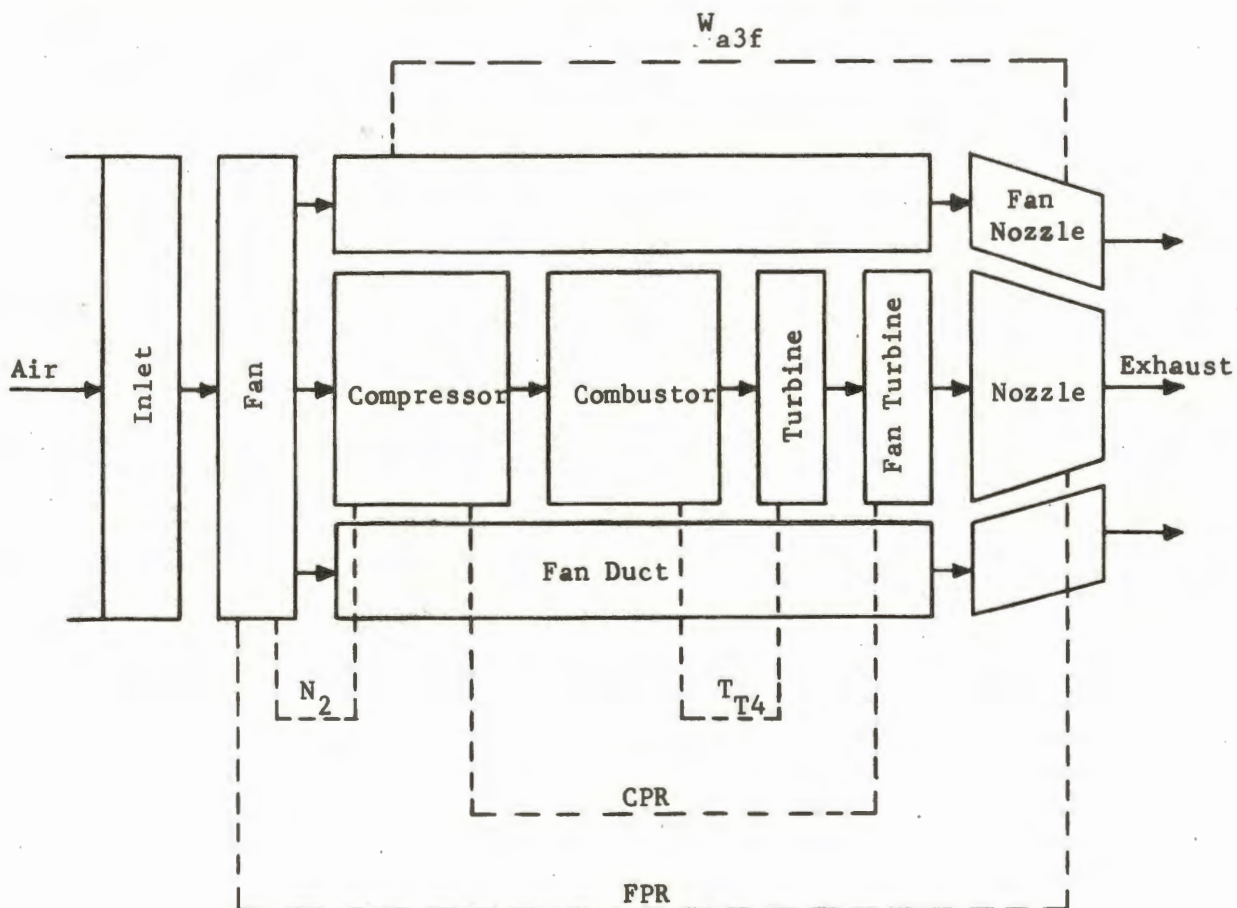


Figure 5. Schematic diagram of front fan turbofan engine with off-design iteration loops.

TABLE II

## FLOW CONTINUITY MATCHES FOR FRONT FAN TURBOFAN ENGINES

MATCH	PARAMETER
Fan exhaust nozzle flow	Bypass airflow, $W_{a3f}$
Compressor flow	Primary rotor speed, $N_2$
Primary turbine flow	Primary turbine inlet total temperature, $T_{T4}$
Fan turbine flow	Primary compressor ratio, CPR
Primary exhaust nozzle flow	Fan pressure ratio, FPR

Off-design engine performance calculations for a front fan turbofan engine can be completed as follows.

Flight conditions. The desired airplane flight condition of altitude, speed, and engine power setting ( $N_1$ ) would be known. The ideal total temperature and pressure are calculated as at design points.

$$T_{T2}/T_{am} = 1 + \frac{\gamma - 1}{2} M_N^2$$

$$P_{T2}/P_{am} = (T_{T2}/T_{am})^{\frac{\gamma}{\gamma-1}}$$

The inlet diffuser efficiency,  $\eta_r$ , is usually a function of flight Mach number so it can be read directly from a curve or calculated by accepted standards.<sup>4</sup> The actual engine inlet total pressure

---

<sup>4</sup>U.S., Military Specification, MIL-E-5008C, December, 1965, p. 4.

and temperature are:

$$P_{T2} = \eta_r (P'_{T2}/P_{am}) P_{am}$$

$$T_{T2} = (T_{T2}/T_{am}) T_{am}$$

Fan. A fan pressure ratio is assumed to start the fan calculations. This pressure ratio is selected as a function of fan referred speed,  $N_1/\sqrt{\theta_{T2}}$ , and flight speed,  $M_N$ , or design bypass ratio, BPR. The fan pressure ratio and referred speed are used to determine the referred fan airflow,  $W_{a2}\sqrt{\theta_{T2}}/\delta_{T2}$ , and efficiency,  $\eta_f$ , from a fan map such as Figure 6. The fan outlet conditions are calculated as for design points using the map values of efficiency and flow.

$$\Delta h'_f = f(\text{FPR}, T_{T2}) \quad (\text{isentropic relationship})$$

$$\Delta h_f = \Delta h'_f / \eta_f$$

$$h_{T2.5} = h_{T2} + \Delta h_f$$

$$T_{T2.5} = f(h_{T2.5})$$

$$P_{T2.5} = P_{T2} (\text{FPR})$$

$$W_{a2} = (W_{a2}\sqrt{\theta_{T2}}/\delta_{T2}) \delta_{T2}/\sqrt{\theta_{T2}}$$

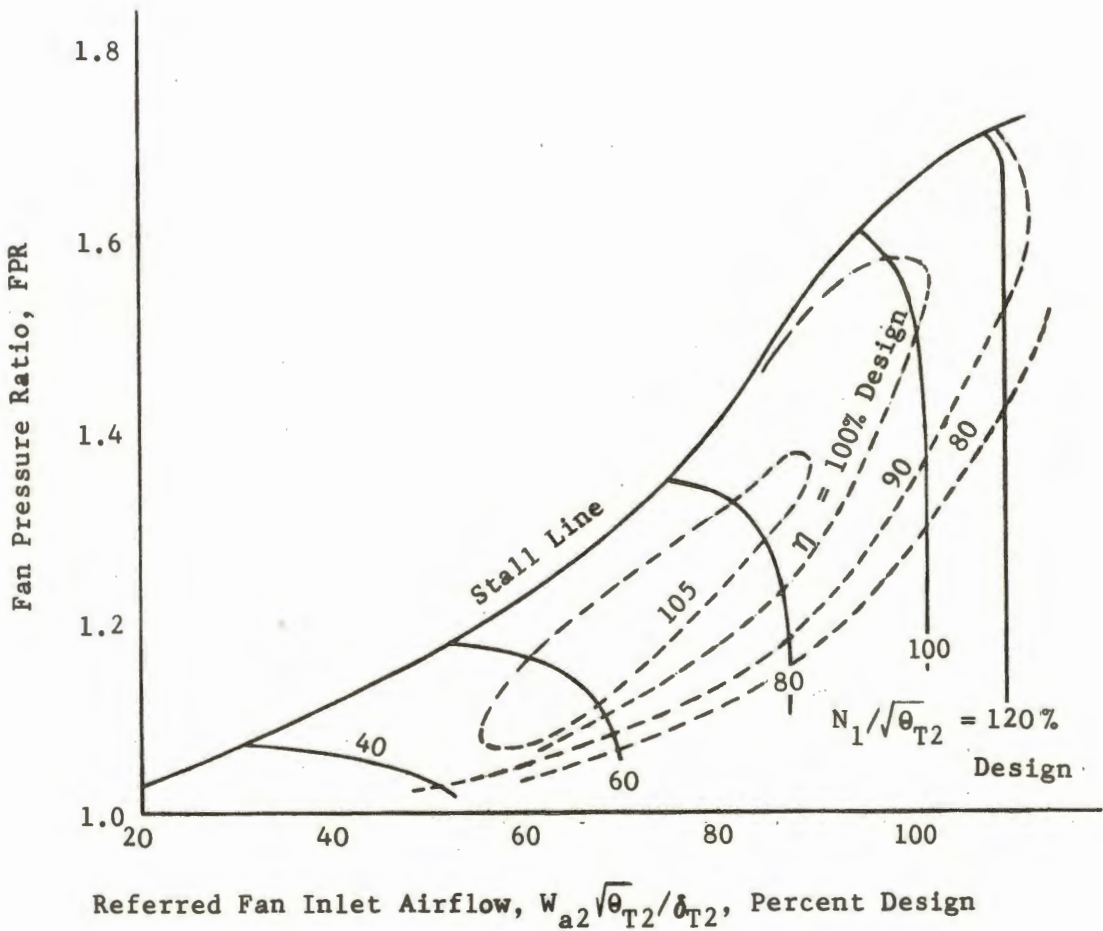


Figure 6. Typical fan performance map

Fan duct-nozzle. The fan duct and nozzle system involves the first of several iterative calculations. The controlling parameter is the nozzle flow relationship which is actually a simple function of the nozzle total to static pressure ratio. Fan duct pressure drop,  $\Delta P_{FD}$ , is the only change in thermodynamic properties. This pressure drop is essentially determined by Fanno line relationships<sup>5</sup>

<sup>5</sup>Ivan H. Driggs and Otis E. Lancaster, Gas Turbines for Aircraft, page 184.

but can be approximated by

$$\Delta P_{FD}/P_{T3f} = K_{FD} \Gamma_{T3f}^2$$

$K_{FD}$  is determined at the design point.

The initial value of  $\Gamma_{T3f}$ ,  $W_{a3f} \sqrt{\theta_{T2.5}}/\delta_{T2.5}$ , is determined by assuming no fan duct pressure drop and calculating the nozzle flow. This flow is then used iteratively to determine the nozzle inlet total pressure, nozzle flow, etc., until the flow value becomes constant. Fan exhaust nozzle thrust is calculated as it is for design points.

Compressor. The compressor air flow is established as the remainder of the fan flow after the fan nozzle is satisfied.

$$W_{a2.5} = W_{a2} - W_{a3f}$$

$$\Gamma_{T2.5} = W_{a2.5} \sqrt{\theta_{T2.5}}/\delta_{T2.5}$$

This referred compressor flow,  $\Gamma_{T2.5}$ , and an assumed operating line are used to select initial values of inner spool speed,  $N_2$ , and compression ratio, CPR. This CPR is maintained constant and the compressor map flow is adjusted by varying rpm until the fan outlet flow is matched. A compressor performance map similar to Figure 7 is used to determine this flow match and operating efficiency.<sup>6</sup> Compressor outlet conditions are calculated as for the design point using the map variables.

---

<sup>6</sup>Ray E. Budinger and Arthur R. Thomson, Investigation of a 10-Stage Subsonic Axial-Flow Research Compressor; II-Preliminary Analysis of Over-All Performance, NACA RM E52C04, p. 15.

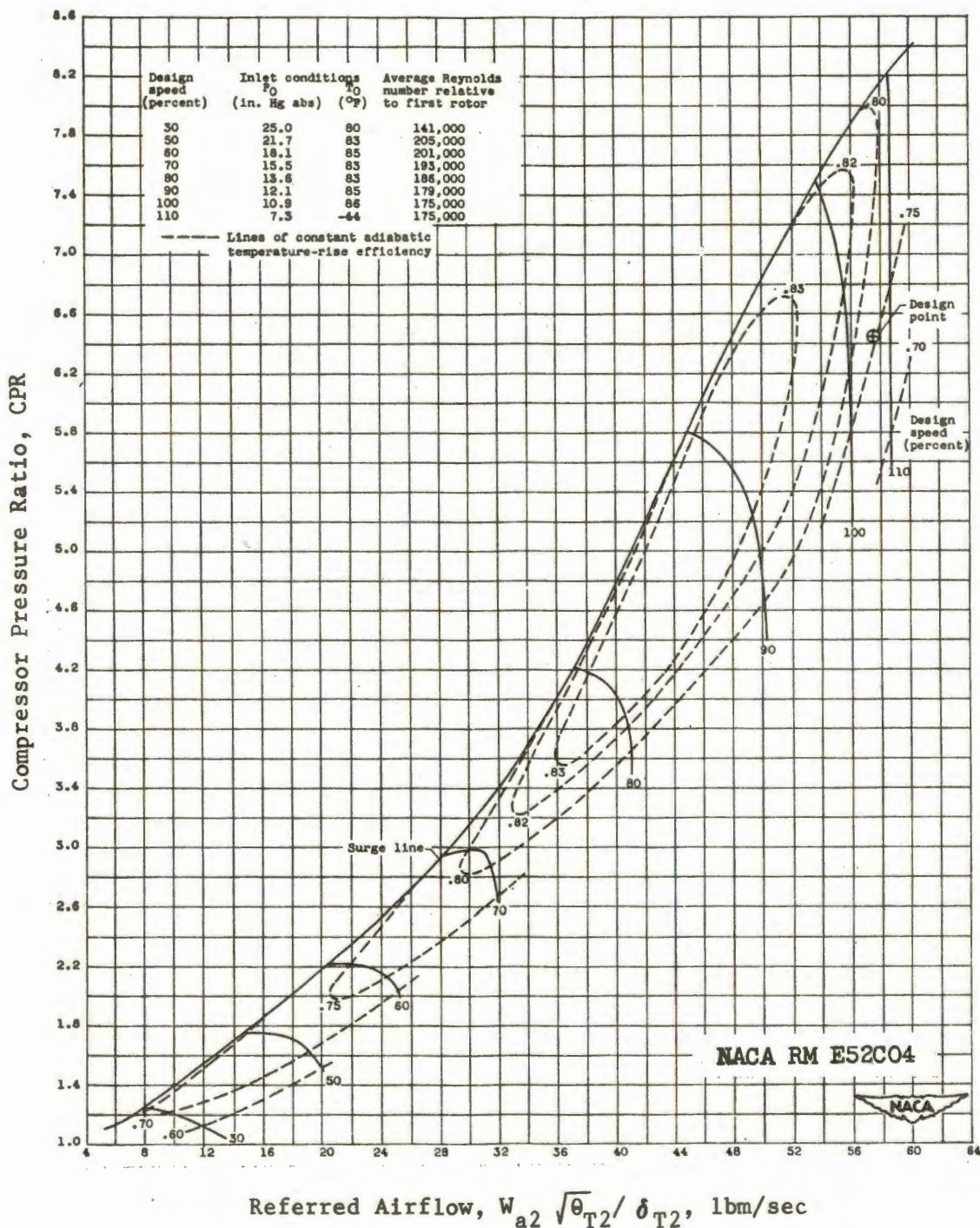


Figure 7. 10-stage axial-flow compressor performance

Combustor. Combustor inlet flow,  $W_{a3}$ , and the total temperature,  $T_{T3}$ , are the compressor outlet conditions. The combustion efficiency,  $\eta_B$ , is nearly constant over a wide range of burning conditions so it can be assumed constant. At very low Reynolds' number flow, the combustion efficiency has been correlated as a function of  $P_{T3} T_{T3} / V_B$  and the fuel air ratio,  $W_f / W_a$ .

The fuel air ratio is calculated by an energy balance for an assumed turbine inlet total temperature,  $T_{T4}$ . This temperature is changed iteratively to satisfy the turbine flow parameter.

The combustor pressure drop,  $\Delta P_B$ , is best calculated by a combination of Fanno and Rayleigh line relationships. However, for low section flow Mach numbers and moderate heat addition, it can be approximated by

$$\Delta P_B / P_{T3} = K_B \Gamma_{T3}^2$$

$K_B$  is evaluated at the design point.

Turbine. Since the turbine and compressor are coupled, the turbine work is determined from the compressor work, and turbine speed is equal to compressor speed. The turbine pressure ratio is determined from the turbine work by the isentropic relationships and an assumed efficiency. The referred turbine work,  $\Delta h_t / \theta_{cr4}$ , and pressure ratio are used to determine the true efficiency and required referred flow from a turbine map like Figure 8.<sup>7</sup> Two iterations are required to

---

<sup>7</sup> Warner L. Stewart, Robert Y. Wong, and David G. Evans, Design and Experimental Investigation of Transonic Turbine With Slight Negative Reaction Across Rotor Hub, NACA RM E53L29a, p. 34.

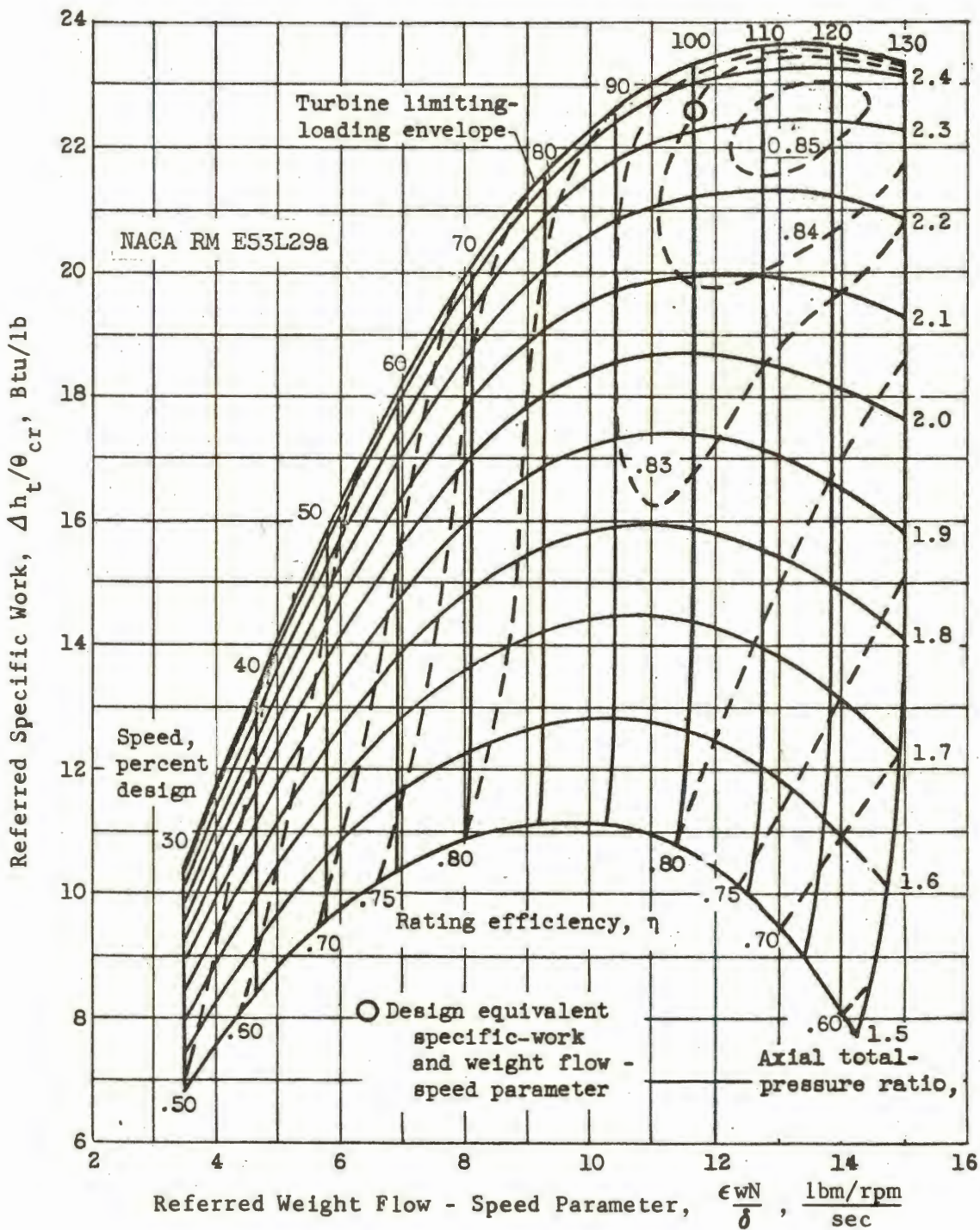


Figure 8. Turbine performance map

satisfy the turbine efficiency and flow rate. The efficiency iteration is easily completed by merely using the map value. The flow parameter is adjusted by varying the turbine inlet temperature and iterating through the combustor and turbine. The turbine outlet flow rate and gas properties are determined during the turbine iteration.

Fan turbine. The fan turbine performance is determined similarly to the primary turbine except that the primary compression ratio, CPR, is the iterative variable. This loop requires satisfying the internal iterations on  $N_2$  and  $T_{T4}$ .

Primary exhaust nozzle. The primary exhaust nozzle flow must be satisfied by the fan turbine outlet flow. Therefore, this final iteration, encompassing all the internal loops, is completed by adjusting fan pressure ratio, FPR, until the nozzle flow function is matched.

This final match completes the off-design point calculation because all the components are satisfied and all assumptions are substantiated.

External performance. Once the operating matches are completed, the external performance is calculated as if the engine were at a design condition.

A sample cycle calculation is presented on the enthalpy-entropy chart of Figure 9. This chart shows the specific enthalpy, specific entropy and pressure variation around a 1.5 BPR front fan turbofan engine operating at off-design conditions.

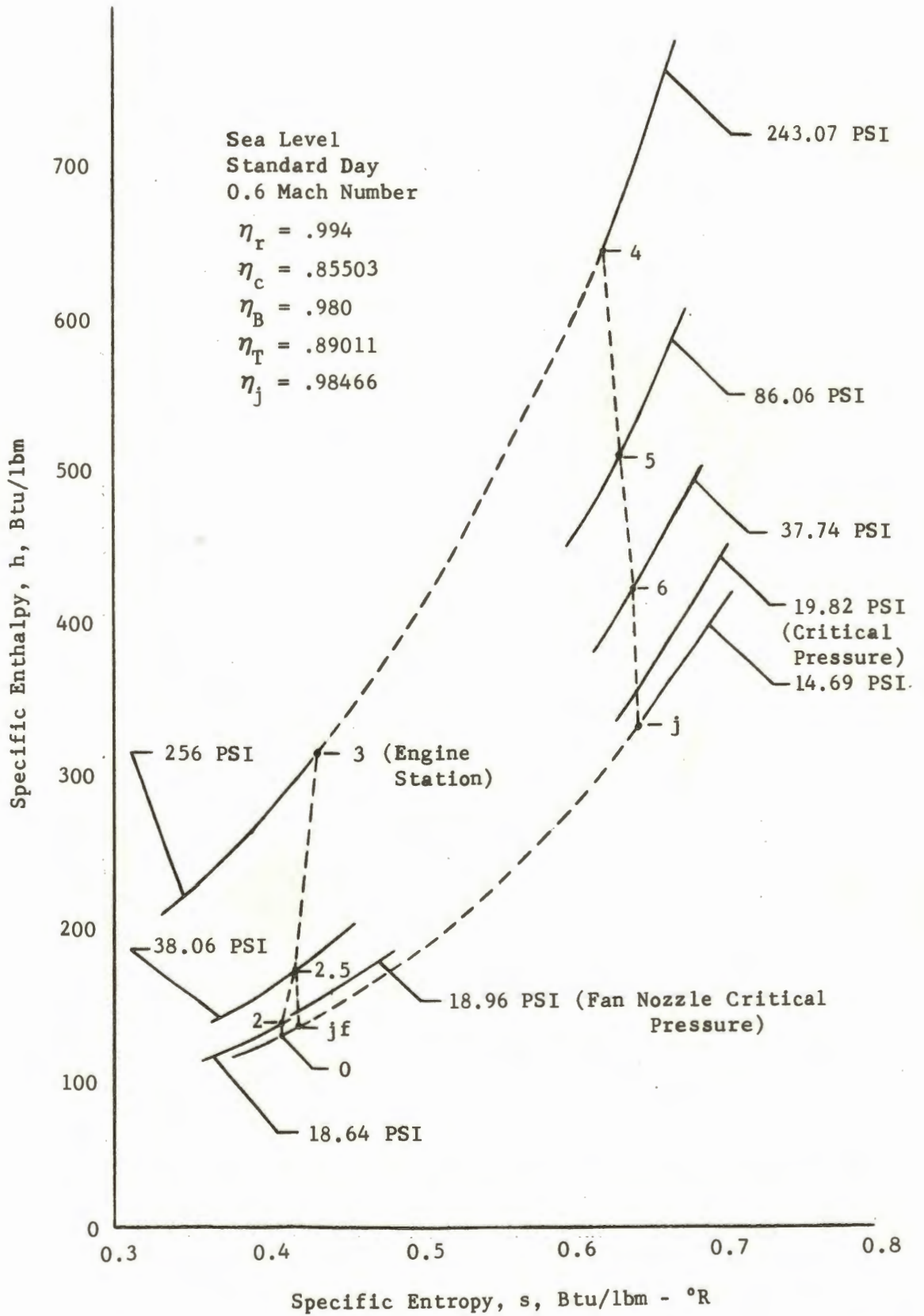


Figure 9. Front fan turbofan cycle presented on enthalpy-entropy diagram

## CHAPTER III

### ENGINE COMPONENT CHARACTERISTICS

#### Fan and Compressors

Axial flow and centrifugal compressor performance is usually presented on graphs similar to Figures 6 and 7 of Chapter II. These plots, called maps, are determined by testing the individual compressors throughout their speed operating range with various back pressures. The map provides the mass flow parameter and adiabatic efficiency as functions of the compression ratio and referred speed up to the stall line. Additional axial flow compressor maps with design pressure ratios of approximately 8.0 and 9.0 are shown on Figures 10 and 11.<sup>1</sup> The similarities of these three compressor maps are apparent.

Experience has shown that within reasonable limits of design pressure ratio, compressor maps can be ratioed to a common design pressure ratio for comparison. This ratioing is accomplished by simple arithmetic ratios of the speed, flow and efficiency and logarithmic ratio of the pressure ratio. That is:

---

<sup>1</sup>Richard P. Geye, Ray E. Budinger, and Charles H. Voit, Investigation of a High Pressure Ratio Eight-Stage Axial-Flow Research Compressor with Two Transonic Inlet Stages, NACA RM E53J06, p. 15; Raymond M. Standahar and Richard P. Geye, Investigation of a High-Pressure-Ratio Eight-Stage Axial-Flow Research Compressor with Two Transonic Inlet Stages; V-Preliminary Analysis of Over-all Performance of Modified Compressor, NACA RM E55A03, p. 14.

$$\% \text{ Flow} = (W \sqrt{\theta_T} / \delta_T) / (\text{Design } W \sqrt{\theta_T} / \delta_T)$$

$$\text{Ln Pressure Ratio} = (\text{Ln Map Pressure Ratio})(\text{Ln Design Pressure Ratio}) / \text{Ln Map Design Pressure Ratio}$$

The flow parameter and stall lines of Figures 7 and 11, ratioed to the design point of Figure 10, are shown on Figure 12 for selected speeds. This figure indicates that compressor map flow and pressure ratio can be generalized. Inspection of the compressor efficiency contours of the three compressor maps indicates their similarities and that the efficiency ratios are comparable. Therefore, the entire compressor map can be ratioed to different design conditions, within limits, and used to study the effects of variations in compressor parameters on engine performance.

The fan map of Figure 6 is an example of generalized performance as it is composed of three NACA maps with design pressure ratios of 1.26, 1.77, and 2.0 ratioed to a design pressure ratio of 1.5.<sup>2</sup> This map is considered adequate to describe fan performance for fans with design pressure ratios from slightly over 1.0 to 2.0. At higher pressure ratios the fan performance would not be representative of an actual fan.

---

<sup>2</sup>Edward R. Tysl, Francis C. Schwenk, and Thomas B. Watkins, Experimental Investigation of a Transonic Compressor Rotor with a 1.5-Inch Chord Length and an Aspect Ratio of 3.0; I-Design, Over-All Performance, and Rotating-Stall Characteristics, NACA RM E54L31, p. 33; James E. Hatch and Daniel T. Bernatowicz, Aerodynamic Design and Over-All Performance of a 24-Inch Two-Spool Transonic Compressor, NACA RM E56L07a, p. 56; John F. Klapproth, John J. Jacklitch, Jr., and Edward R. Tysl, Design and Performance of a 1400-Foot-Per-Second-Tip-Speed Supersonic Compressor Rotor, NACA RM E55A27, p. 32.

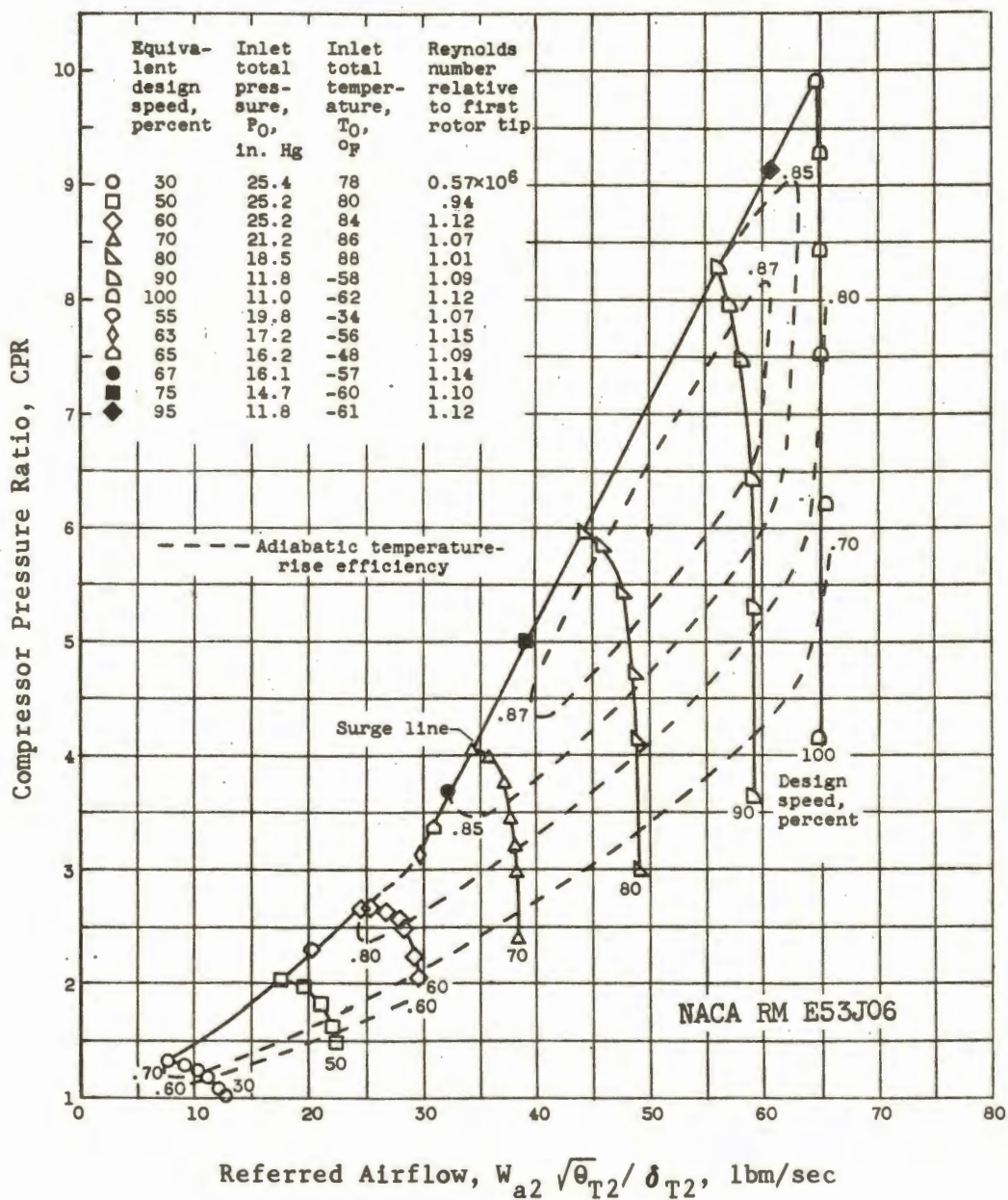


Figure 10. Eight-stage axial-flow compressor map

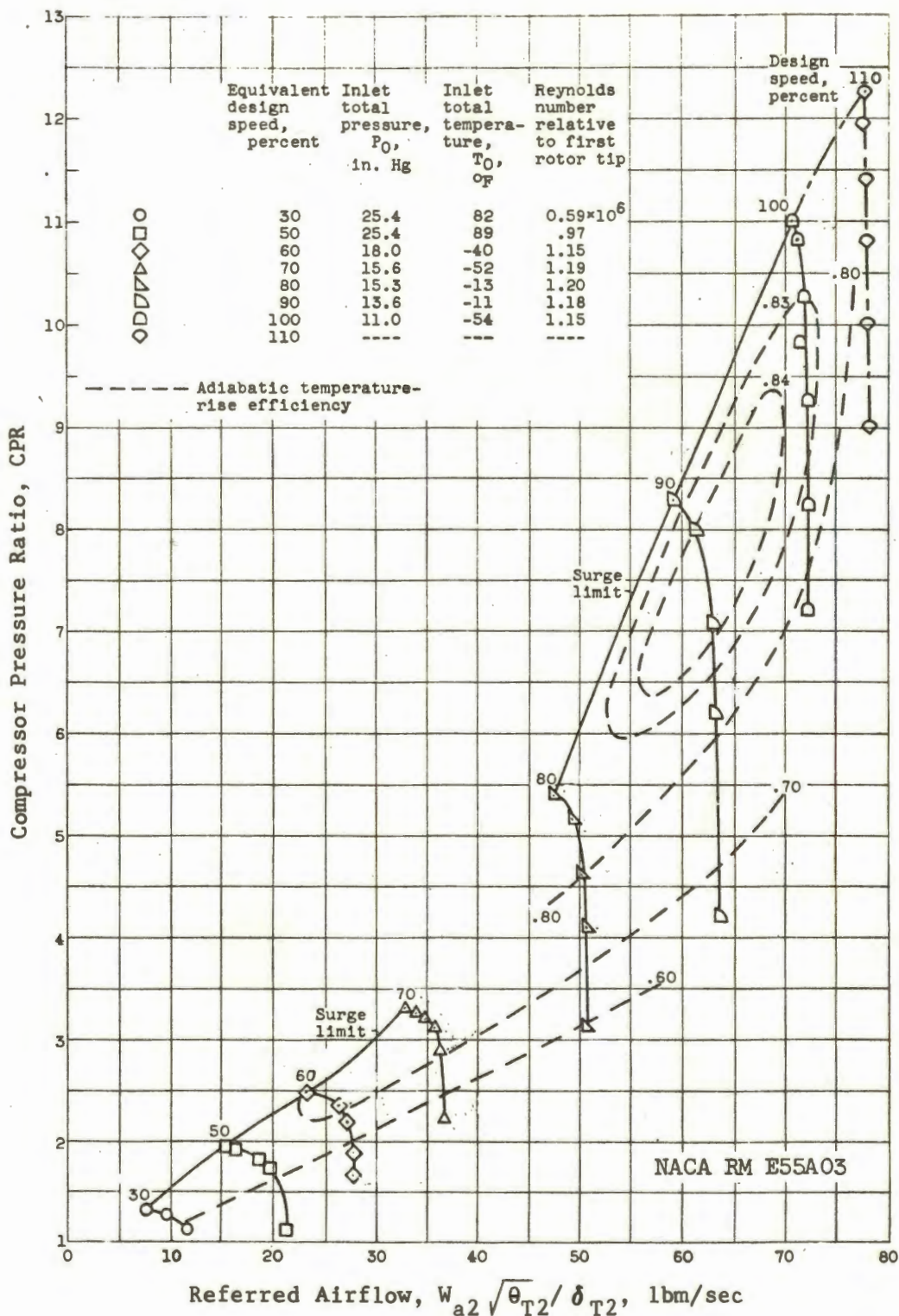


Figure 11. Modified (two transonic stages) eight-stage axial-flow compressor performance

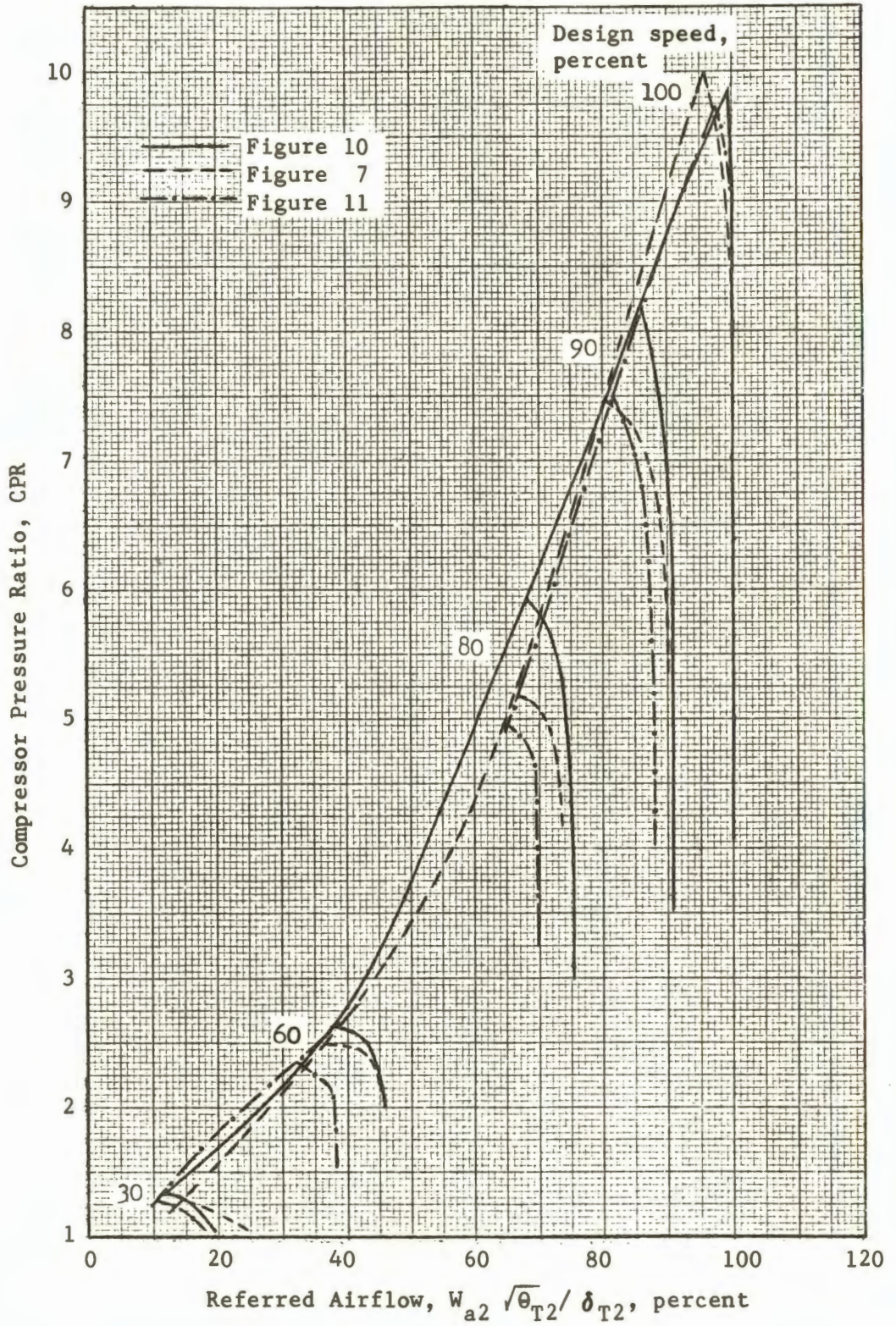


Figure 12. Compressor map comparison

### Combustor

Combustion chamber performance consists of burner efficiency and pressure drop data. Combustion efficiency is usually presented as functions of fuel-air ratio,  $W_f/W_a$ , and the combustor parameter, total pressure times total temperature divided by section velocity,  $P_{T3}T_{T3}/V_B$ .<sup>3</sup> Figure 13 is a typical burner efficiency graph for combustion of gasoline with air. Fuel-air ratios are not specified on this curve. Above moderate values of the combustor parameter, the burner efficiency is essentially constant. This region includes sea level and low altitude operation at higher engine power settings.

Combustor pressure drop consists of friction and momentum pressure losses. These losses are usually presented as functions of the referred airflow,  $W_{a3} \sqrt{\theta_{T3}} / \delta_{T3}$ , and burner temperature ratio,  $T_{T4}/T_{T3}$ .<sup>4</sup> Since the temperature ratio varies approximately with the flow parameter, this second variable is superfluous.

Generalized combustor performance for preliminary design calculations could be:

1. Constant combustion efficiency.
2. Pressure drop varying as the flow parameter squared.

---

<sup>3</sup> J. Howard Childs and Charles C. Graves, Relation of Turbine-Engine Combustion Efficiency to Second-Order Reaction Kinetics and Fundamental Flame Speed, NACA E54G23, p. 25.

<sup>4</sup> Ivan H. Driggs and Otis E. Lancaster, Gas Turbines for Aircraft, pp. 176-194.

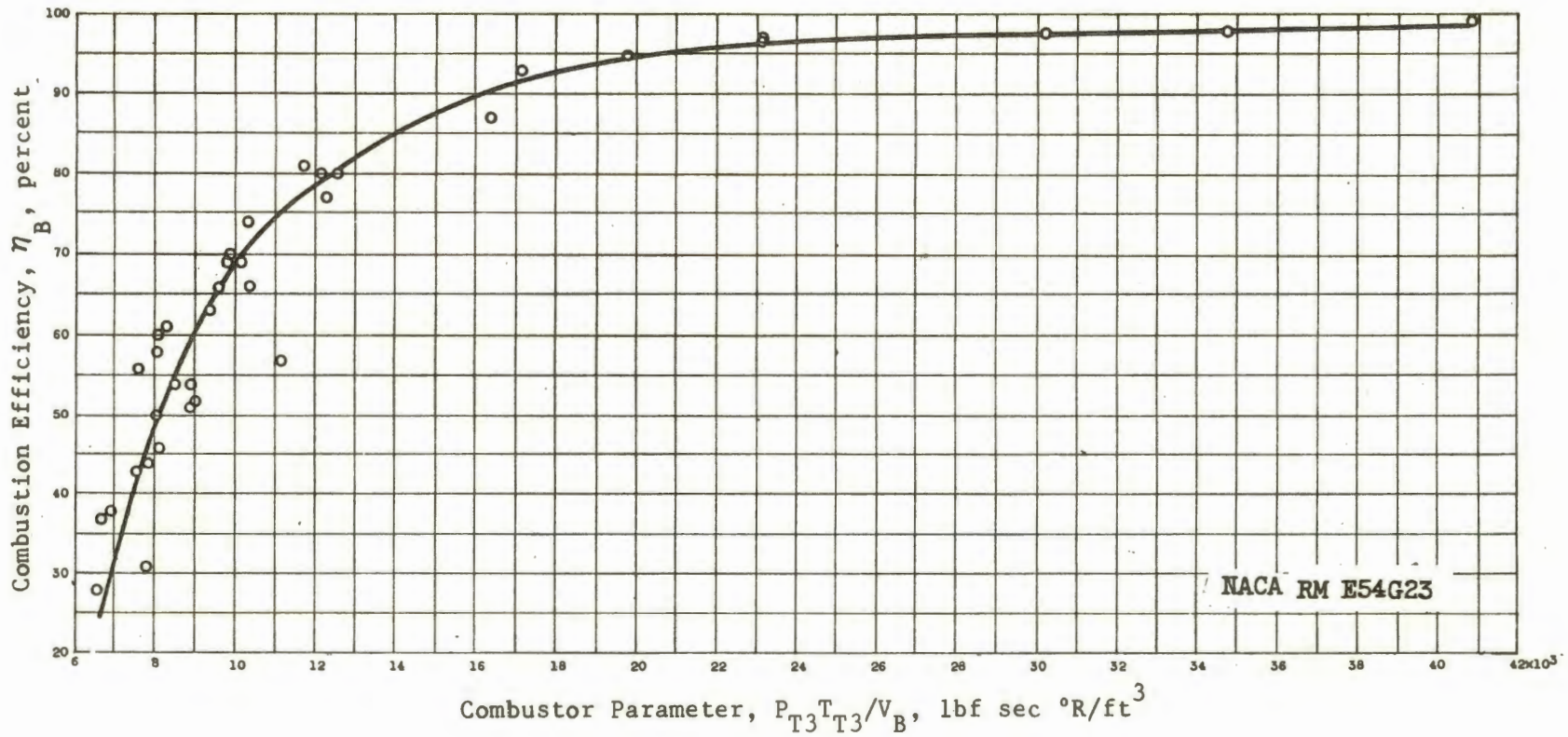


Figure 13. Experimental combustor data for gasoline burned in air with various fuel-air ratios

## Turbines

The turbine performance maps shown on Figures 8 and 14 are typical test results taken from the unclassified NACA literature.<sup>5</sup> These figures show referred specific work output, total pressure ratio, and adiabatic efficiency as functions of referred speed and referred flow. Both these maps are plotted versus a referred flow-speed parameter. This parameter includes the referred speed to spread the variable's range and accent the slight difference in referred flow.

Inspection of these turbine maps reveals that:

1. Both turbines choke (referred flow constant) at moderate total pressure ratios (1.6 and 1.4) that are relatively insensitive to speed.
2. The efficiency contours of the maps are similar.
3. The flow parameter is practically constant for a fixed pressure ratio.

These performance trends can be generalized and presented in simplified form by separating the flow and efficiency parameters. The flow parameter is analogous to the simple nozzle flow parameter and can be plotted versus a pressure ratio parameter as the sample of Figure 15,

$$W \sqrt{\theta}_T \text{ in} / \delta_T \text{ in} A' V_s (P_{T \text{ in}}/P_{T \text{ out}})^{-1} / (P_{T \text{ in}}/P_{T \text{ out}})_{\text{choke}}^{-1} .$$

Turbine efficiency can be plotted as a ratio of design point efficiency versus referred speed and a referred work parameter. This

---

<sup>5</sup> Stewart, Wong, and Evans, loc. cit.; Warner L. Stewart, Investigation of Rotating Components of Counterrotating Two-Spool Engines; I-Analytical Investigation of Off-Design Performance of Turbine Component Designed with and without Outer-Turbine Stator, NACA RM E54J13, p. 20.

work parameter is the ratio of turbine work to the maximum possible turbine work at that referred speed. Figure 16 presents a turbine work limit curve and Figure 17 illustrates the generalized turbine efficiency plot.

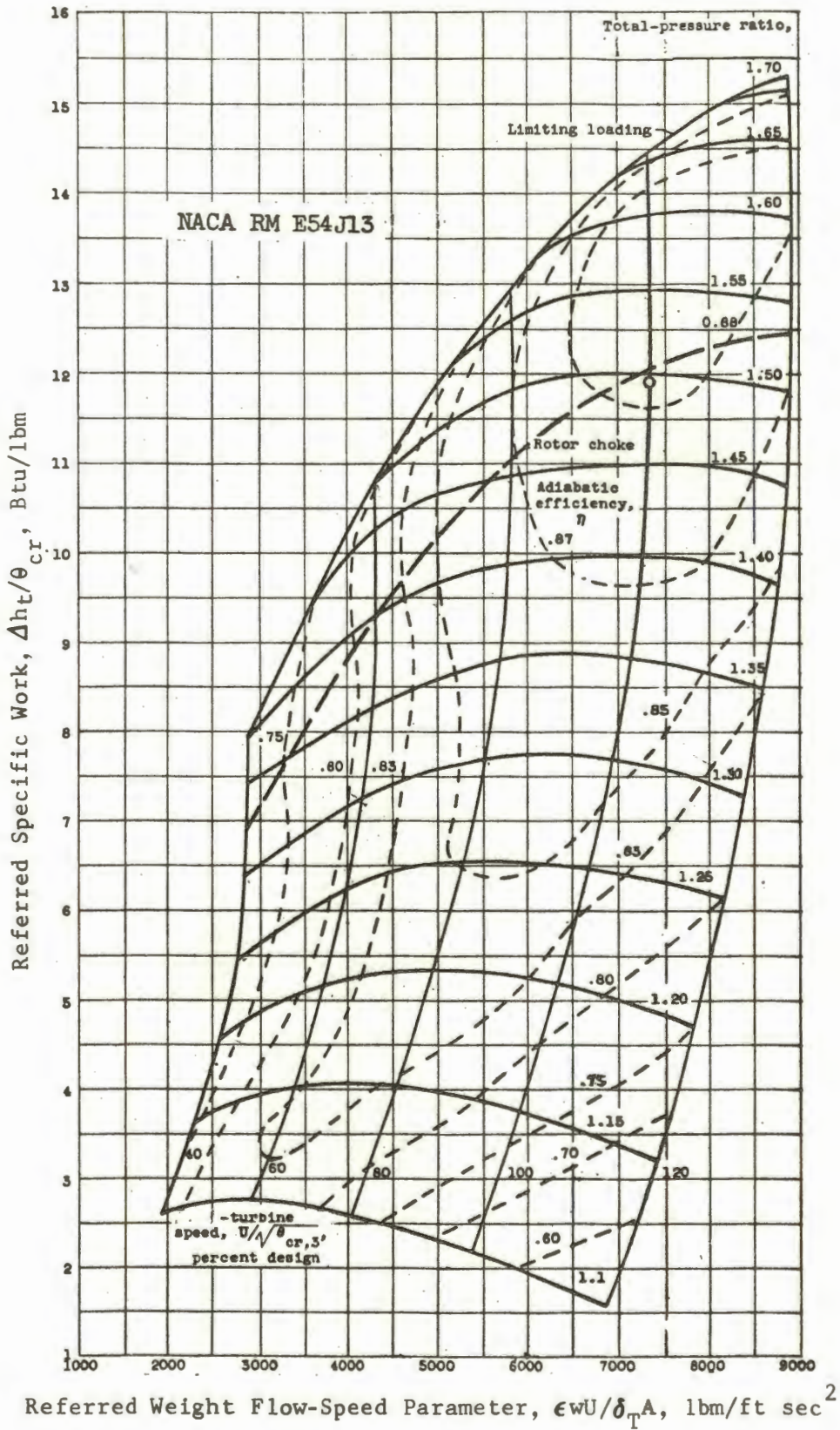


Figure 14. Turbine performance map

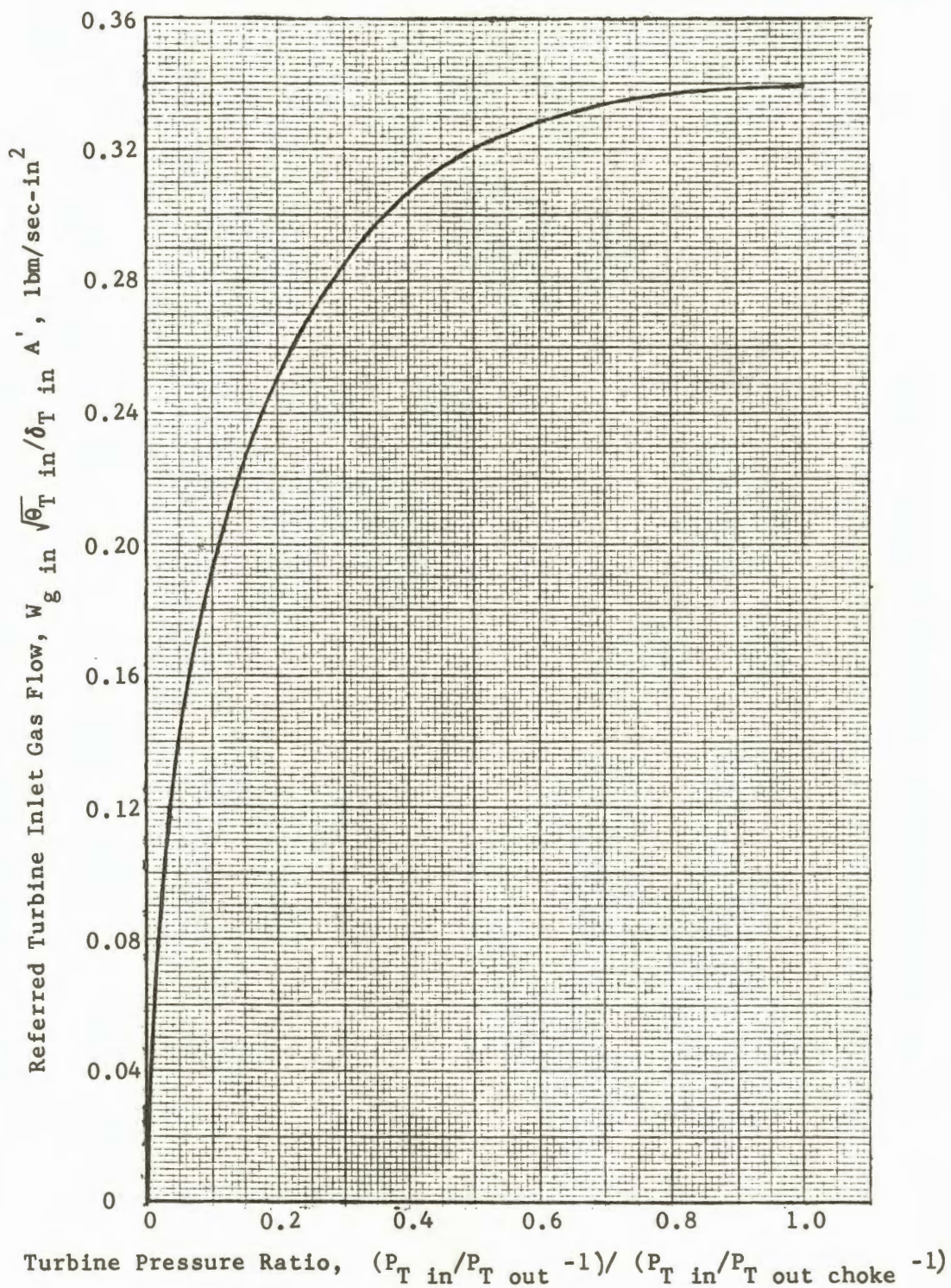


Figure 15. Turbine flow characteristic

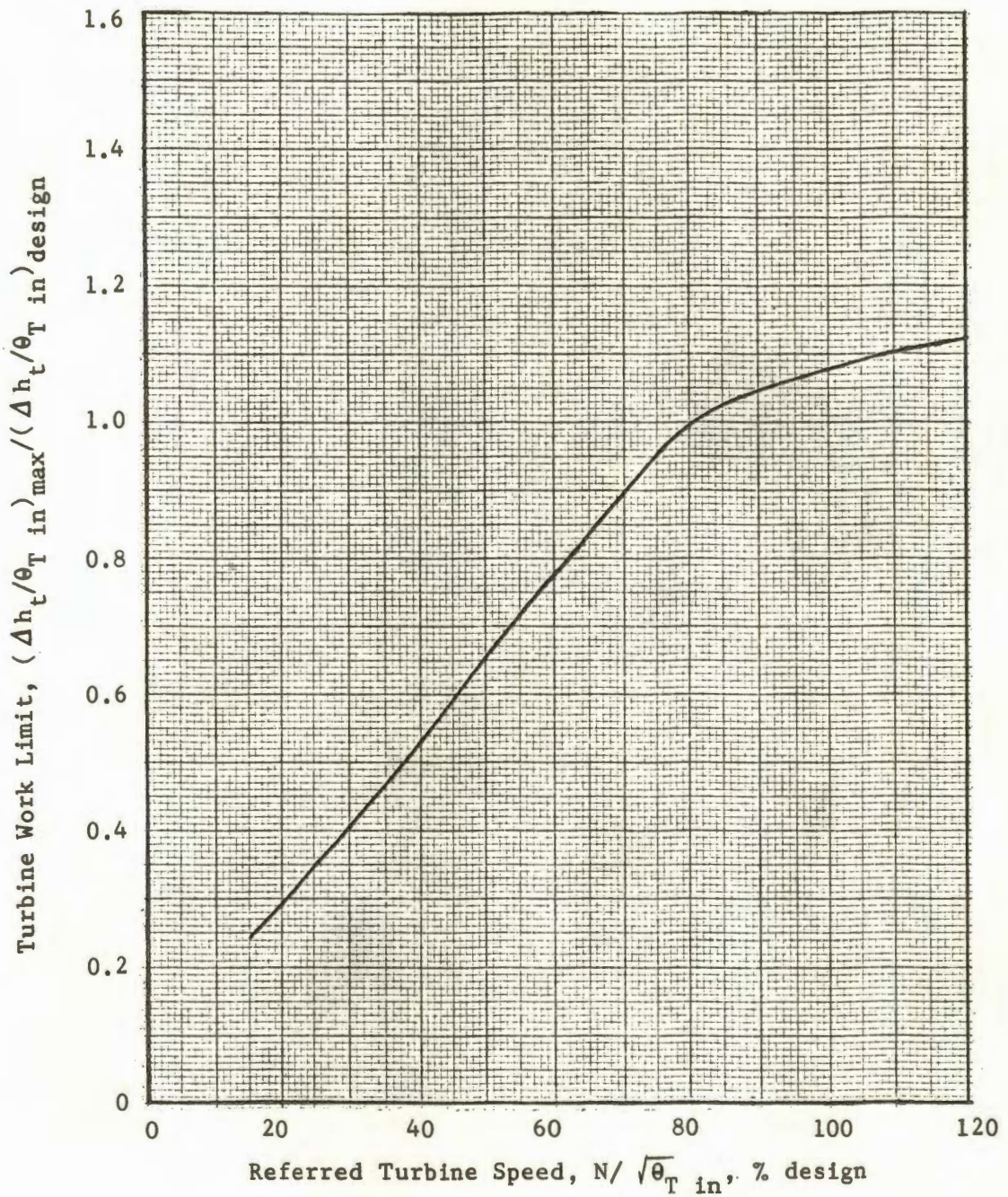


Figure 16. Turbine work limit

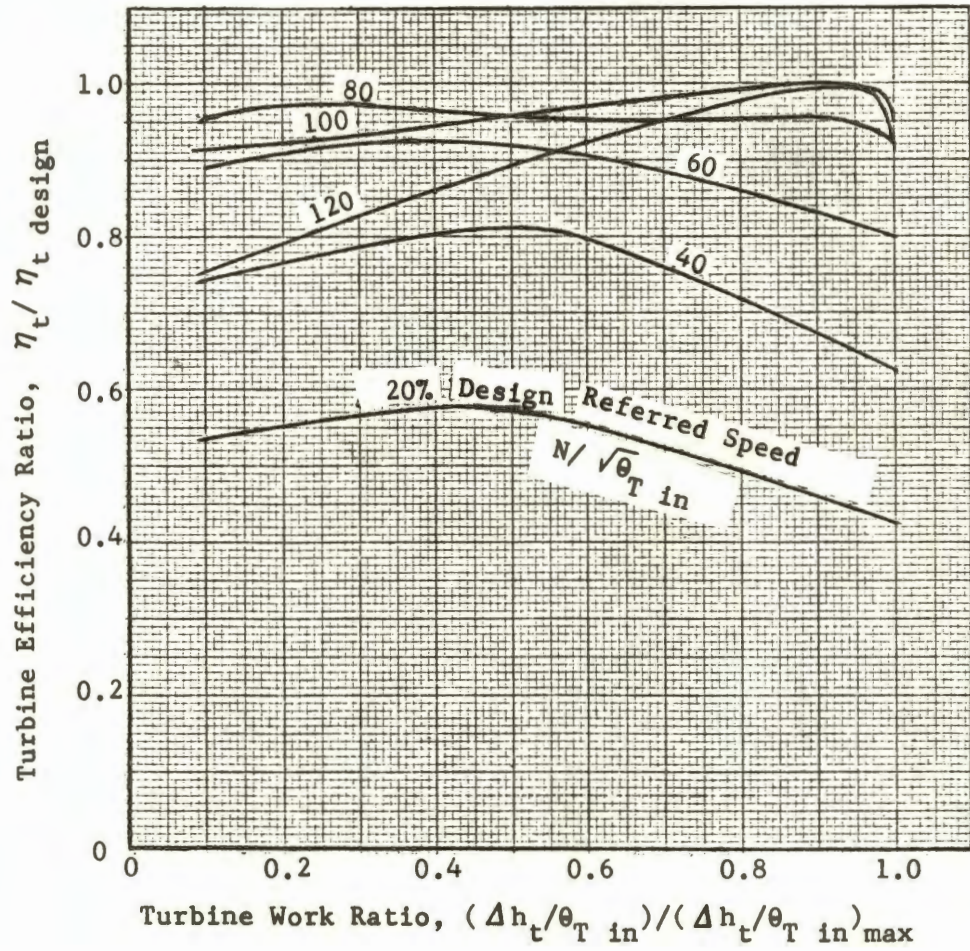


Figure 17. Turbine efficiency

## CHAPTER IV

### GENERALIZED COMPUTER PROGRAM

#### Description

A generalized gas turbine engine performance computer program has been developed. This program determines turbine engine performance by the methods of Chapter II using the generalized fan, compressor, combustor, and turbine maps of Chapter III with specific inlet and exhaust routines. The computer program ratios the fan, compressor and turbine performance maps to the desired design point and uses them for off-design calculations.

At off-design conditions the fan performance is determined from the generalized map as follows. The referred fan speed,  $N_1 / \sqrt{\theta_{T2}}$ , is calculated from the input and known conditions. FPR is known by assumption or at a value required to complete the cycle. The percent of design referred speed is

$$\% N_1 / \sqrt{\theta_{T2}} = 100 (N_1 / \sqrt{\theta_{T2}}) / (N_1 / \sqrt{\theta_{T2}})_{\text{design}}$$

The map value of FPR is calculated from

$$(FPR)_{\text{map}} = \text{Antilog} (\text{Ln}(FPR) \times$$

$$\text{Ln}(FPR)_{\text{map design point}} / \text{Ln}(FPR)_{\text{design point}})$$

The percent design referred airflow and percent design efficiency are read from the map as functions of the percent design referred

speed and map FPR. Thus,

$$\eta_f = (\% \eta_{\text{map}}) \eta_{\text{design point}}$$

and  $W_{a2} \sqrt{\theta_{T2}} / \delta_{T2} = (\% W_{a2} \sqrt{\theta_{T2}} / \delta_{T2})_{\text{map}} \times$

$$(W_{a2} \sqrt{\theta_{T2}} / \delta_{T2})_{\text{design point}}$$

Compressor performance is determined in a similar manner.

To facilitate computer operations, a new pressure ratio parameter is defined. This parameter,  $Q$ , is used to develop a continuous table that is not truncated by the stall line. This parameter, defined between zero and one, is

$$Q = (\text{FPR} - 1) / (\text{FPR}_{\text{stall}} - 1).$$

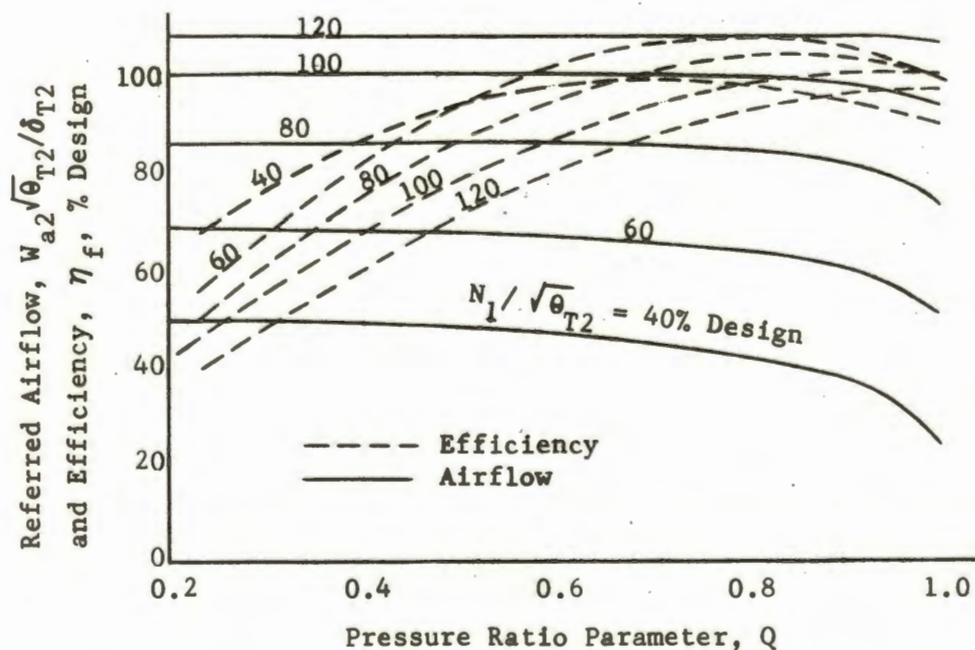


Figure 18. Typical fan performance map presented with pressure ratio parameter

$FPR_{stall}$  is determined at the same referred speed as that of the FPR. The generalized fan map of Figure 6 is presented as a function of the pressure ratio parameter in Figure 18.

The computer calculations for the turbine are completed in the following manner. Turbine inlet temperature, specific work, and rotor speed are known so the referred turbine speed and work are calculated. The maximum referred turbine work is determined from the design point referred turbine work and Figure 16 at the referred speed. Percent design turbine efficiency is read from Figure 17 at the referred turbine work ratio and percent design referred speed. Efficiency is calculated as

$$\eta_t = (\% \eta_{design}) \eta_{t \text{ design point}}$$

This turbine efficiency is used with the actual work and isentropic relationships to determine the turbine total pressure ratio. Referred turbine inlet gas flow is determined from this pressure ratio, the choking pressure ratio and effective turbine nozzle flow area. The referred turbine flow is matched with the combustor outlet flow by varying the combustion temperature.

The remaining computer program routines are merely mechanizations of the standard calculations and the iteration loops discussed in Chapter II. The thermodynamic properties and isentropic flow relationships are determined by polynomial equations derived by curve fitting the gas tables.<sup>1</sup> Iteration loops are closed by:

---

<sup>1</sup>Keenan and Kaye, op. cit., pp. 1-93.

1. Linearly ratioing the independent variable (e.g., CPR) by the variation in the dependent variable (e.g., fan turbine flow).
2. Substitution of a calculated result for an assumed value (e.g., fan nozzle flow).

### Verification

This method of calculating gas turbine engine performance from generalized component characteristics has been verified by matching the performance of hardware engines. Engines from two manufacturers with extreme cycles were selected for comparison purposes. Engine "A" is a recent high bypass ratio front fan engine and engine "B" is an older low bypass ratio aft fan turbofan engine from a different manufacturer. Salient design point features of these engines are listed in Table III.

The generalized computer program results for sea level, standard day conditions are superimposed on the engine manufacturers' data on Figures 19 and 20. These results for both engines match extremely well for cruise conditions and are optimistic for static operation. Since these hardware engines must meet performance ratings at static conditions, manufacturers usually derate their performance for the test conditions. Therefore, the optimistic computer program results are to be expected because they simulate actual test data.

TABLE III

HARDWARE TURBOFAN ENGINE DESIGN POINT DATA  
SEA LEVEL, STATIC, STANDARD DAY

Engine	A	B
Type	Front Fan	Aft Fan
Thrust Class, lbf	40,000	15,000
Bypass ratio	4.96	1.49
Fan pressure ratio	1.52	1.55
Total compression ratio	22.00	12.35
Turbine inlet temperature, °F.	2,000	1,700
Fan efficiency	0.88	0.85
Compressor efficiency	0.84	0.82
Combustion efficiency	0.98	0.98
Combustor pressure drop, %	5.00	5.00
Primary turbine efficiency	0.90	0.90
Fan turbine efficiency	0.90	0.90
Fan duct pressure drop, %	3.00	0
Fan nozzle velocity coefficient	0.985	0.98
Primary nozzle velocity coefficient	0.98	0.98

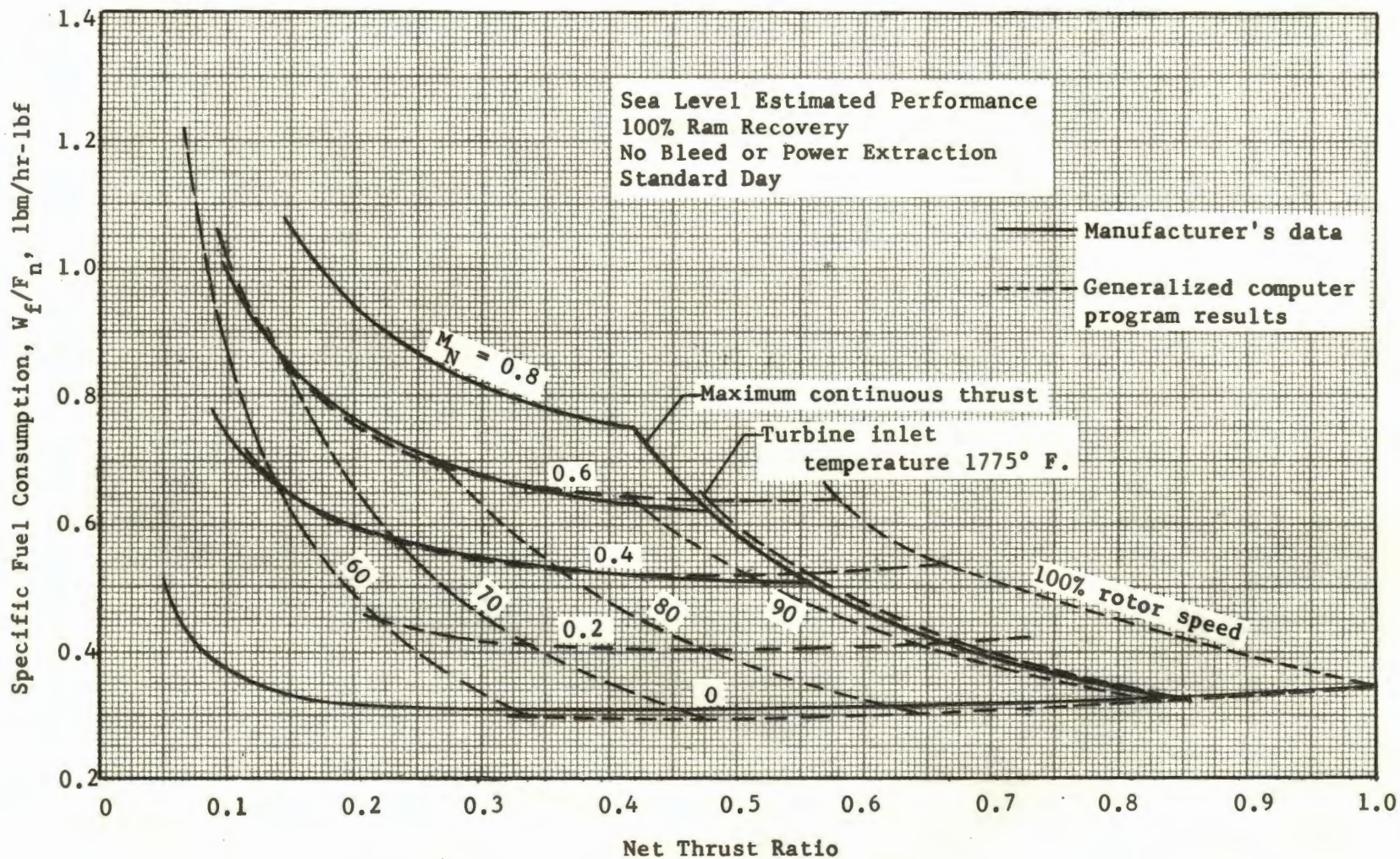


Figure 19. Engine "A" (front fan) sea level performance

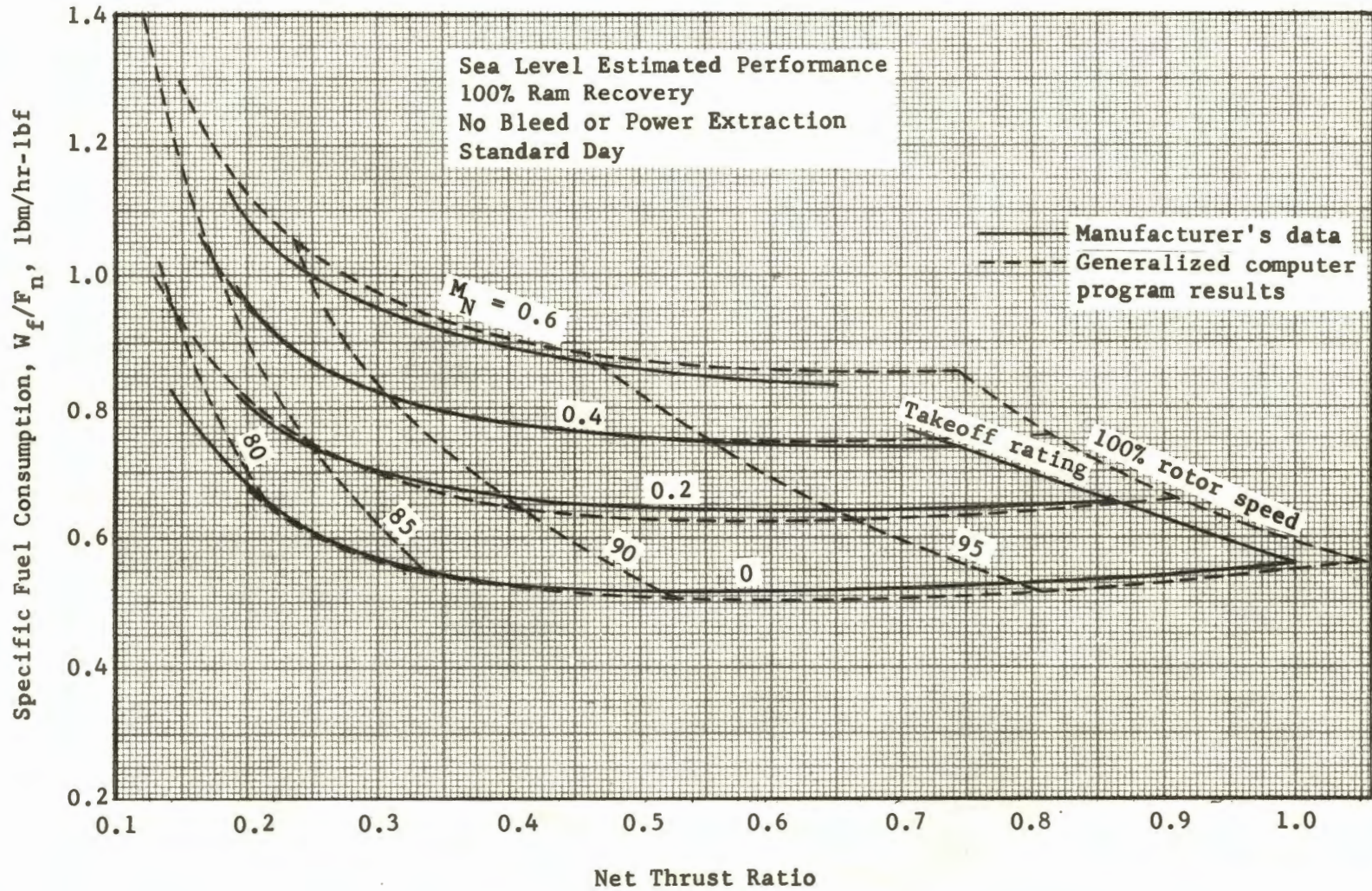


Figure 20. Engine "B" (aft fan) sea level performance

## Results

The engine performance data for the turbojet and turbofan engines of Figures 1 and 2 were calculated with the generalized gas turbine performance computer program. Fixed design point data for these engines is presented in Table IV, and the individual engine data significant sizing constants derived at the design point are listed in Table V. These data and the program verification results indicate the utility and versatility of a generalized turbine engine performance computer program.

TABLE IV

DESIGN POINT DATA OF STUDY ENGINES  
SEA LEVEL, STATIC, STANDARD DAY

Total compression ratio	20.0
Turbine inlet temperature, °F.	2000.0
Primary airflow, lbm/sec	1.0
Fan efficiency	0.85
Compressor efficiency	0.85
Combustion efficiency	0.98
Combustor pressure drop, %	5.0
Primary turbine efficiency	0.90
Fan turbine efficiency	0.90
Fan duct pressure drop, %	3.0
Fan nozzle velocity coefficient	0.98
Primary nozzle velocity coefficient	0.98

TABLE V

INDIVIDUAL DESIGN POINT DATA AND SIZING CONSTANTS OF STUDY ENGINES  
SEA LEVEL, STATIC, STANDARD DAY

Engine	1	2	3	4
Bypass ratio	-	2	4	6
Total airflow, lbm/sec	1.0	3.0	5.0	7.0
Fan pressure ratio	-	2.0	1.6	1.4
Primary net thrust, lbf	83.523	59.683	50.447	48.534
Total net thrust, lbf	83.523	130.49	163.41	188.18
Specific fuel consumption, lbm/hr-lbf	0.807	0.508	0.408	0.355
Turbine nozzle throat area, sq in	0.3439	0.3439	0.3439	0.3439
Fan turbine nozzle throat area, sq in	-	1.0754	1.1616	1.12126
Primary jet nozzle area, sq in	1.3838	2.4881	2.9840	3.1051
Fan jet nozzle area, sq in	-	3.4669	8.5865	15.510
Combustor pressure drop constant, $\text{sec}^2/\text{lbm}^2$	7.8815	7.7656	7.7945	7.8157
Fan duct pressure drop constant, $\text{sec}^2/\text{lbm}^2$	-	0.0239	0.00411	0.00146

## CHAPTER V

### CONCLUSIONS

Based on the preceding discussion, data from bibliography references, and computer program results, the following conclusions may be drawn:

1. Compressor and turbine performance data can be presented on generalized maps and ratioed to desired design point values.
2. Simplified duct flow pressure drop coefficients and constant combustion efficiency are reasonable assumptions for a generalized engine performance computer program.
3. Parametric turbine aircraft engine performance can be calculated from generalized engine component data with sufficient accuracy to determine optimum engine size and cycle for given airplane missions.
4. A generalized gas turbine engine performance computer program is an extremely useful tool for an aircraft manufacturer because it will provide:
  - a. Low cost, accurate, parametric engine data in quantity required for an airplane-engine matching study.
  - b. A rapid means of checking performance data of proposed engines to determine its credibility, the

manufacturer's veracity and state-of-the-art component performance.

- c. The effects of installation parameters (inlet and exhaust duct losses, air bleed, shaft power extraction, etc.) on the engine performance.
5. Additional studies of extreme engine components should be completed to determine similarities and differences, and therefore their possible generalization. Specific studies should be completed on:
    - a. Compressors - centrifugal, mixed centrifugal - axial, and supersonic.
    - b. Compressors - axial flow with various stage loading - long and short chord blades.
    - c. Turbines - impulse and various percent reaction.
  6. Reynolds' number effects on engine and component performance should be generalized. Emphasis should be on small engines at extreme altitudes (low Reynolds' number).

## BIBLIOGRAPHY

### BOOKS

Durham, Franklin P. Aircraft Jet Power Plants. New York: Prentice-Hall, Inc., 1951.

Driggs, Ivan H., and Otis E. Lancaster. Gas Turbines for Aircraft. New York: The Ronald Press Co., 1955.

Keenan, Joseph H., and Joseph Kaye. Gas Tables - Thermodynamic Properties of Air Products of Combustion and Component Gases. New York: John Wiley and Sons, Inc., 1960.

Liepmann, Hans Wolfgang, and Allen E. Puckett. Introduction to Aerodynamics of a Compressible Fluid. New York: John Wiley and Sons, Inc., 1947.

Perkins, Courtland D., and Robert E. Hage. Airplane Performance Stability and Control. New York: John Wiley and Sons, Inc., 1949.

### BOOKS: PARTS OF SERIES

Hawthorne, W. R. (ed.). Aerodynamics of Turbines and Compressors. Vol. X of High Speed Aerodynamics and Jet Propulsion. 12 vols. Princeton, New Jersey: Princeton University Press, 1964.

Zucrow, M. J. Thermodynamics of Fluid Flow and Application to Propulsion Engines. Vol. I of Aircraft and Missile Propulsion. 3 vols. New York: John Wiley and Sons, Inc., 1958.

\_\_\_\_\_. The Gas Turbine Power Plant, the Turboprop, Turbojet, Ramjet, and Rocket Engines. Vol. II of Aircraft and Missile Propulsion. 3 vols. New York: John Wiley and Sons, Inc., 1958.

### PUBLICATIONS OF THE GOVERNMENT

Budinger, Ray E., and Arthur R. Thomson. Investigation of a 10-Stage Subsonic Axial-Flow Research Compressor. II - Preliminary Analysis of Over-All Performance. NACA RM E52C04. Washington: National Advisory Committee for Aeronautics, June 16, 1952.

- \_\_\_\_\_, George K. Serovy. Investigation of a 10-Stage Subsonic Axial-Flow Research Compressor. IV - Individual Stage Performance Characteristics. NACA RM E53C11. Washington: National Advisory Committee for Aeronautics, April 28, 1953.
- Childs, J. Howard, and Charles C. Graves. Relation of Turbine-Engine Combustion Efficiency to Second-order Reaction Kinetics and Fundamental Flame Speed. NACA RM E54G23. Washington: National Advisory Committee for Aeronautics, August 24, 1954.
- Felix, A. Richard. Investigation of a High-Flow Transonic-Compressor Inlet Stage Having a Hub-Tip Radius Ratio of 0.35. NACA RM L58A08. Washington: National Advisory Committee for Aeronautics, March 6, 1958.
- Geye, Richard P., Ray E. Budinger, and Charles H. Voit. Investigation of a High-Pressure-Ratio Eight-Stage Axial-Flow Research Compressor with Two Transonic Inlet Stages. II - Preliminary Analysis of Over-All Performance. NACA RM E53J06. Washington: National Advisory Committee for Aeronautics, December 1, 1953.
- \_\_\_\_\_, and Charles H. Voit. Investigation of a High-Pressure-Ratio Eight-Stage Axial-Flow Research Compressor with Two Transonic Inlet Stages. IV - Modification of Aerodynamic Design and Prediction of Performance. NACA RM E55B28. Washington: National Advisory Committee for Aeronautics, June 1, 1955.
- \_\_\_\_\_, and James G. Lucas. Investigation of Effects of Reynolds Number on Over-All Performance of an Eight-Stage Axial-Flow Research Compressor with Two Transonic Inlet Stages. NACA RM E56L11a. Washington: National Advisory Committee for Aeronautics, February 15, 1957.
- Hartmann, Melvin, and Edward R. Tysl. Investigation of a Supersonic-Compressor Rotor with Turning to Axial Direction. II - Rotor Component Off-Design and Stage Performance. NACA RM E53L24. Washington: National Advisory Committee for Aeronautics, March 12, 1954.
- Hatch, James E., and Daniel T. Bernatowicz. Aerodynamic Design and Over-All Performance of First Spool of a 24-Inch Two-Spool Transonic Compressor. NACA RM E56L07a. Washington: National Advisory Committee for Aeronautics, March 4, 1957.
- Jansen, Emmert T., and John E. McAulay. Compressor Performance Characteristics of a Python Turbine-Propeller Engine Investigated in Altitude Wind Tunnel. NACA RM E50K24. Washington: May 1, 1951.

Klapproth, John F., Guy N. Ullman, and Edward R. Tysl. Performance of an Impulse-Type Supersonic Compressor with Stators. NACA RM E52B22. Washington: National Advisory Committee for Aeronautics, April 28, 1952.

\_\_\_\_\_, John J. Jacklitch, Jr., and Edward R. Tysl. Design and Performance of a 1400-Foot-per-Second-Tip-Speed Supersonic Compressor Rotor. NACA RM E55A27. Washington: National Advisory Committee for Aeronautics, April 11, 1955.

Lown, Harold, and Melvin J. Hartmann. Investigation of a 24-Inch Shock-in-Rotor Type Supersonic Compressor Designed for Simple Radial Equilibrium Behind Normal Shock. NACA RM E51H08. Washington: National Advisory Committee for Aeronautics, December 12, 1951.

Savage, Melvyn, and Loren A. Beatty. Investigation of a Three-Stage Transonic Research Axial-Flow Compressor; Aerodynamic Design and Overall Performance. NACA RM L55G27. Washington: National Advisory Committee for Aeronautics, October 27, 1955.

Schacht, Ralph L., Arthur W. Goldstein, and Harvey E. Neumann. Performance of a Supersonic Rotor Having High Mass Flow. NACA RM E54D22. Washington: National Advisory Committee for Aeronautics, July 19, 1954.

Schwenk, Francis C., Seymour Lieblein, and George W. Lewis, Jr. Experimental Investigation of an Axial-Flow Compressor Inlet Stage Operating at Transonic Relative Inlet Mach Numbers. III - Blade-Row Performance of Stage with Transonic Rotor and Subsonic Stator at Corrected Tip Speeds of 800 and 1000 Feet per Second. NACA RM E53G17. Washington: National Advisory Committee for Aeronautics, September 18, 1953.

Standahar, Raymond M., Morgan P. Hanson, and Richard P. Geye. Investigation of a High-Pressure-Ratio Eight-Stage Axial-Flow Research Compressor with Two Transonic Inlet Stages. VI - Over-All Performance, Rotating Stall, and Blade Vibration at Low and Intermediate Compressor Speeds. NACA RM E55I13. Washington: National Advisory Committee for Aeronautics, November 1, 1955.

\_\_\_\_\_, and Richard P. Geye. Investigation of a High-Pressure-Ratio Eight-Stage Axial-Flow Research Compressor with Two Transonic Inlet Stages. V - Preliminary Analysis of Over-All Performance of Modified Compressor. NACA RM E55A03. Washington: National Advisory Committee for Aeronautics, May 23, 1955.

- Stewart, Warner L. Investigation of Rotating Components of Counter-Rotating Two-Spool Engines. I - Analytical Investigation of Off-Design Performance of Turbine Component Designed with and without Outer-Turbine Stator. NACA RM E54J13. Washington: National Advisory Committee for Aeronautics, January 10, 1955.
- \_\_\_\_\_, Robert Y. Wong, and David G. Evans. Design and Experimental Investigation of Transonic Turbine with Slight Negative Reaction Across Rotor Hub. NACA RM E53L29a. Washington: National Advisory Committee for Aeronautics, March 12, 1954.
- Tysl, Edward R., John F. Klapproth, and Melvin J. Hartmann. Investigation of a Supersonic-Compressor Rotor with Turning to Axial Direction. I - Rotor Design and Performance. NACA RM E53F23. Washington: National Advisory Committee for Aeronautics, August 19, 1953.
- \_\_\_\_\_, Francis C. Schwenk, and Thomas B. Watkins. Experimental Investigation of a Transonic Compressor Rotor with a 1.5-Inch Chord Length and an Aspect Ratio of 3.0. I - Design, Over-All Performance, and Rotating-Stall Characteristics. NACA RM E54L31. Washington: National Advisory Committee for Aeronautics, March 28, 1955.
- U.S. Military Specification. Engines, Aircraft, Turbojet and Turbofan, Model Specifications For. MIL-E-5008C. Washington: U.S. Government Printing Office, December 30, 1965.
- Vanco, Michael R. Computer Program for Design-Point Performance of Turbojet and Turbofan Engine Cycles. NASA Technical Memorandum TM X-1340. Washington: National Aeronautics and Space Administration, February, 1967.
- Voit, Charles H., and Richard P. Geye. Investigation of a High-Pressure-Ratio Eight-Stage Axial-Flow Research Compressor with Two Transonic Inlet Stages. III - Individual Stage Performance Characteristics. NACA RM E54H17. Washington: National Advisory Committee for Aeronautics, November 1, 1954.
- Walker, Curtis L., and Emmert T. Jansen. Performance Investigation and High-Flight-Speed Application of a Turbine with a Variable-Area Stator. NACA RM E54G26a. Washington: National Advisory Committee for Aeronautics, October 25, 1954.
- Wilcox, Ward W. Investigation of Impulse-Type Supersonic Compressor with Hub-Tip Ratio of 0.6 and Turning to Axial Direction. II - Stage Performance with Three Different Sets of Stators. NACA RM E55F28. Washington: National Advisory Committee for Aeronautics, August 16, 1955.

\_\_\_\_\_, and Linwood C. Wright. Investigation of Two-Stage Counter-Rotating Compressor. I - Design and Over-All Performance of Transonic First Compressor Stage. NACA RM E56C15. Washington: National Advisory Committee for Aeronautics, May 22, 1956.

#### PERIODICALS

- Holeski, D. E., and W. L. Stewart. "Study of NASA and NACA Single-Stage Axial Flow Turbine Performance as Related to Reynolds Number and Geometry," Transactions of the ASME, Journal of Engineering for Power, July, 1964, pp. 296-298.
- Rodgers, Colin. "Typical Performance Characteristics of Gas Turbine Radial Compressors," Transactions of the ASME, Journal of Engineering for Power, April, 1964, pp. 161-175.
- Serovy, G. K. "Recent Progress in Aerodynamic Design of Axial-Flow Compressors in the United States," Transactions of the ASME, Journal of Engineering for Power, July, 1966, pp. 251-261.

